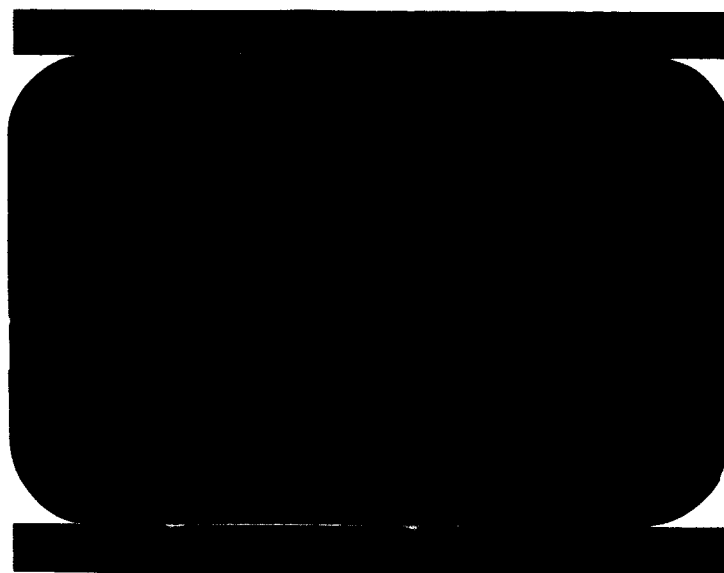


C 2



FACILITY FORM 505
N-66-22244
93
44
93
CR-67213
93
13

(THRU)
/ (CODE)
28 (CATEGOR)

GPO PRICE \$ _____

CFSTI PRICE(S) \$ _____

Hard copy (HC) 3.00

Microfiche (MF) .75

653 July 65



GIHIIIIID

GENERAL DYNAMICS
ASTRONAUTICS

JUL 18 1962

ENTER
A
ION
IDA



A2136-1 (REV. 6-61)



THE USE OF A COAXIAL GUN FOR
PLASMA PROPULSION

R. H. Lovberg, B. Hayworth, T. Gooding

FINAL REPORT

CONTRACT NAS-5-1139

May 15, 1962

Lewis Research Center
National Aeronautics and Space Administration
21000 Brookpark Road,
Cleveland 35, Ohio

GMIIIIID

GENERAL DYNAMICS | ASTRONAUTICS

TABLE OF CONTENTS

<u>Section</u>	<u>Page No.</u>
A. Introduction.	1
B. Choice of Circuit Parameters.	10
C. Mode of Gun Operation	16
D. Experimental Program.	18
E. Magnetic Probes	18
F. Electric Probes	21
G. Experimental Devices and Results.	24
1. Mark I.	24
2. Mark II	38
3. Mark III.	51
4. Ballistic Pendulum Measurements	59
5. Mark IV	64
6. Repetitive Firing Experiments	65
7. Recharging Bank	72
H. <u>Discussion and Conclusions</u>	75
Appendix I.	80
Appendix II	83
Appendix III.	85
Appendix IV	88
References.	89

LIST OF FIGURES

<u>Figure</u>	<u>Page No.</u>
1. Schematic of an Induction Accelerator.	8
2. Mark I Coaxial Gun	25
3. The Electrical System.	27
4. Gas Valve Pulsing Circuit.	28
5. Cross Section of the Gas Valve	30
6. Distribution of B_{θ} , E_z for the Mark I Gun.	33
7. Distribution of B_{θ} , E_z for the Mark I Gun.	34
8. Ion Density Distributions.	35
9. Time Distributions of B_{θ} and E_z for the Mark I Gun . . .	36
10. Mark II Gun.	39
11. Mark II Gun.	40
12. Mark II Gun.	41
13. Mark II Gun.	42
14. Mark II Gun.	43
15. Cross Section of the Mark II, III, IV Guns	44
16. The Insulator Assembly	43
17. Distributions of B_{θ} , E_z for the Mark II Gun.	50
18. Distributions of B_{θ} and E_z for the Mark III Gun.	52
19. Time Distribution of B_{θ} and E_z	54
20. Time Distribution of B_{θ} and E_z	54a
21. Time Distribution of the Intensity of the 4094 Angstrom Line	56

LIST OF FIGURES (CON'T)

<u>Figure</u>		<u>Page No.</u>
22.	The Plasma Velocity Determined from the Monochromator Data.	57
23.	The Position of the Current Sheet	58
24.	Time Distribution of the Total Current I, and B_{θ}	60
25.	The Pendulum Arrangement.	61
26.	The Mark IV Gun	66
27.	The Experimental Arrangement.	67
28.	The Vacuum System	68
29.	The Control Panel and Screened Room	69
30.	The Electrical Schematic of the Condenser Bank.	73
31.	The Condenser Bank	74
32.	The B Probe	81
33.	The E Probe	84
34.	The E Probe Isolation Transformer	87

THE USE OF A COAXIAL GUN FOR PLASMA PROPULSION

R. H. Lovberg, B. Hayworth, T. Gooding

A. Introduction

In the extension of space flight planning to interplanetary missions, it has become clear that present propulsion systems, i.e., chemical rockets, are adequate only to send very small payloads to these regions. The lofting of anything as heavy as a manned vehicle, together with fuel sufficient for a planetary orbit or landing and return to earth, would involve unacceptably large take-off weights and sizes. This can be seen most easily by writing the simple differential equation of motion for a rocket which we suppose to be already in a low orbit, but accelerating toward escape energy. Concerning the momentum of the vehicle-propellant system, we have,

$$M \frac{dv_r}{dt} + v_e \frac{dM}{dt} = 0 ,$$

where

v_e = exhaust velocity,

v_r = vehicle velocity,

M = total rocket mass.

This immediately integrates to

$$\Delta v_r = v_e \ln \frac{M_0}{M_1} ,$$

where M_0 and M_1 are the initial and final rocket masses, respectively.

This equation tells us that if we seek a velocity increment substantially larger than the rocket exhaust velocity, our starting mass is almost entirely fuel; further, the situation gets exponentially worse as the velocity increment, in units of v_e , increases. Clearly, the salvation of the problem lies in going to higher exhaust velocities. Enormous effort has gone into the search

for fuels which react energetically and expel products of low molecular weight. As can be seen from our rocket equation, the rewards, in terms of flyable payload, for even slight improvements in v_e can be very great. Nevertheless, there appears to be a fairly firm upper limit on the v_e attainable in chemical reactions which is well below that necessary for manned flight to other planets.

We introduce here a parameter characterizing the rocket system which is called specific impulse, I_{sp} . It is defined as the ratio of thrust (F) to mass-flow rate, and when, in the engineering tradition, we measure both force and mass in units of pounds, I_{sp} is in units of seconds. However, if we use physical units of dynes thrust and grams mass, the ratio becomes just the exhaust velocity v_e in cm/sec. The connecting relationship is $v_e = I_{sp} \cdot g$.

In these terms, then, we find that the best chemical fuels yield specific impulse in the range of 400 - 500 seconds. Thus, a velocity increment of 5 miles per second, which one might wish to add to orbital velocity in order to proceed towards Mars, would require a fuel load fraction of about 80%, and the weight after burnout would itself be mostly fuel in the case of a manned vehicle which would have to return again to earth. However, if we increase I_{sp} to 1,000 seconds, this fuel load fraction drops to just over one half and for 2,000 seconds it is about one third. In the limit of high I_{sp} , one obtains

$$\Delta M = M_0 \cdot \frac{\Delta v_r}{v_e},$$

and so the fuel load could, in principle, become negligible.

The production of these high exhaust speeds forces a resort to other than thermo-chemical means, since no thermal speed obtainable from such reactions is great enough. An intermediate step of considerable value is to raise the temperature of exhaust gases by such means as electric arcs or passage through a high-power nuclear reactor. Here, one may make use of very light gases such as hydrogen, and thus obtain maximum thermal speed for a given temperature. I_{sp} values in the neighborhood of 1,000 are obtainable by this means. Nevertheless, one ultimately encounters the obstacle of

material failure at high temperatures, and so this procedure is also limited.

Finally, we arrive at electromagnetic acceleration of matter in an ionized, charged, or conducting state. Here, there has been a discrete jump past the thermal difficulties mentioned above. The essential point which characterizes electrical propulsion is that it is possible to deposit large translational energy in a propellant without having first gone through a phase of thermal heating. For example, it is quite trivial to build an ion accelerator whose beam "stagnation temperature" is billions of degrees; yet the machine components need not be above room temperature. An equivalent point of view is that the energy imparted to the propellant is not made to undergo equipartition; it remains resident in one degree of freedom, and in this coordinate encounters no material object. (This is only approximately true for some devices.)

Since it is well known that ions may readily be accelerated to relativistic energies, we may inquire if this is not the direction to go; the propellant loss could be made almost arbitrarily low for a given thrust. The objection to this is that the power required is the product of thrust and exhaust velocity, and for too high I_{sp} , the weight of the necessary power supply would become intolerable. Clearly, then, there exists an optimum I_{sp} where the total initial weight of the vehicle, for a given mission and type of power supply is minimum. We may estimate this I_{sp} in the following manner:

$$v_e (= g \cdot I_{sp}) = \frac{F}{\frac{dM_p}{dt}} = \frac{F\tau_m}{M_p},$$

where M_p is the propellant mass expelled at constant rate and velocity v_e over a mission time τ_m .

The beam power is

$$P_e = Fv_e.$$

We define the "specific mass" (α) of the power supply as the mass (M_{ps}) per unit power output, and we also relate electrical power (P_o) to

beam power (P_e) by an efficiency ϵ ; thus,

$$\alpha = \frac{M_{ps}}{P_o} = \frac{M_{ps}\epsilon}{P_e} = \frac{M_{ps}\epsilon}{Fv_e}.$$

Now, the total initial mass is

$$\begin{aligned} M_{tot} &= M_{vehicle} + M_p + M_{ps} \\ &= M_v + \frac{F\tau}{v_e} + \frac{Fv_e\alpha}{\epsilon}. \end{aligned}$$

For minimum M_{tot} , we set the derivative with respect to v_e equal to zero, and so obtain

$$v_{e(opt)}^2 = \frac{\epsilon\tau m}{\alpha}.$$

Under this condition,

$$M_p = M_{ps} = F\sqrt{\frac{\tau\alpha}{\epsilon}}$$

There is obviously a premium on high engine efficiency and light power supplies. A less obvious result of this simple relationship is that long missions call for high I_{sp} . More elaborate versions of this calculation modify these answers by numerical constants not far from unity; they show that for missions ranging from lunar to the near planets, and for α in the region of 20 - 50 lbs/kw(e), we are considering I_{sp} values in the 1,000-10,000 second range, or $10^6 < v_e < 10^7$ cm/sec.

In the present work, we have explored a certain area of magneto-hydrodynamic (MHD) acceleration. MHD schemes exploit the bulk electrical conductivity of ionized gases, in that when current (j) is passed through such a "plasma" containing a magnetic field, (B), a body force,

$$\vec{f} = \vec{j} \times \vec{B}$$

is applied to each volume element. We are concerned, in this propulsion application of MHD accelerators, with the efficiency with which the "pushing" of the propellant is done, i.e., we must discover criteria to apply in the system design such that the total acceleration work $\int \mathbf{f} \cdot \mathbf{v} dt$ done on the propellant is a large fraction of the electrical energy supplied to the device. (While one is also concerned with the attainment of correct I_{sp} , it turns out that the efficiency problem is far more difficult and will receive most attention here.)

It is useful for present purposes to employ a rather simple electrical circuit analysis. While it is physically more illuminating to think of the actual plasma acceleration in terms of the fundamental electromagnetic equations, the circuit approach has considerable generality, and further, the correspondence with Maxwell's equations, the Poynting vector, etc., are easily established.

In these terms, then, a pulsed MHD accelerator may be thought of as an inductive (and resistive) circuit into which one applies a pulse of current, usually from a charged capacitor. It is always true that the magnetic forces on an inductor are such as to increase its inductance. In our case, a portion of this circuit, having some mass associated with it, is allowed to move; in fact, these expanding current elements are the plasma, and so we have built an accelerator. At the terminals of such a circuit, the voltage is given by

$$V = IR + \frac{d\phi}{dt},$$

where ϕ is the total magnetic flux threading the circuit. By the definition of inductance, this becomes

$$\begin{aligned} V &= IR + \frac{d}{dt} (LI) \\ &= IR + L \frac{dI}{dt} + I \frac{dL}{dt} . \end{aligned}$$

The input power is

$$P = VI = I^2 R + LI \frac{dI}{dt} + I^2 \frac{dL}{dt}.$$

In order to separate the three right-hand terms functionally, we first decompose the second term:

$$LI \frac{dI}{dt} = \frac{d}{dt} \left(\frac{LI^2}{2} \right) - \frac{I^2}{2} \frac{dL}{dt}.$$

Then,

$$P = I^2 R + \frac{d}{dt} \left(\frac{LI^2}{2} \right) + \frac{1}{2} I^2 \frac{dL}{dt}.$$

Now, these three terms represent distinct power inputs. The first, clearly, is the resistive heat loss in the circuit. Since $LI^2/2$ is the total magnetic field energy in any inductance, the second term is just the rate of gain of this energy. The third term is the rate of work done on the moving boundary, and for an accelerator is evidently the term into which we wish to dump as much input energy as possible.

If one has, for the acceleration impulse, some certain quantity of energy W_0 , (e.g., $\frac{1}{2} CV_0^2$ for a capacitor) we can examine the fate of this energy by integrating the power equation over the time of the impulse. Note first that the integral of the second term is zero, since the impulse begins and ends with zero magnetic field. Hence,

$$W_0 = \int I^2 \left(R + \frac{1}{2} \frac{dL}{dt} \right) dt.$$

The system efficiency may now be defined as

$$\epsilon \equiv \frac{\frac{1}{2} \int I^2 L dt}{W_0}.$$

We may carry this a step farther for cases where the peak current depends upon the circuit inductance, e.g., for capacitive or inductive energy storage. In these cases, $I_{\max} < I_0$, where I_0 is the peak current

which would have been achieved if L had been held constant, and if also there had been no resistive losses. That is, $W_0 = \frac{1}{2} L_0 I_0^2$, where L_0 is the initial system inductance. Then,

$$\epsilon = \frac{\int I^2 L \cdot dt}{L_0 I_0^2}$$

$$< \frac{\int I_0^2 L \cdot dt}{L_0 I_0^2} = \frac{\Delta L}{L_0}$$

We see, then, that the system efficiency is limited by the relative inductance change which has occurred during the acceleration. If this ratio is still small when the electromagnetic energy has vanished in the system, we are assured that most of the energy has been wasted as heat, and is not directed beam energy.

While we have assumed, in the above analysis, that we are dealing with an impulsive system, the treatment is general enough to cover both the case of an inductively driven plasma, in which a current loop induced in the plasma is repelled from the primary coil, and the "rail gun" which may be a rail pair, parallel plates, or coaxial cylinders.

Both of these schemes possess certain technical advantages and disadvantages. The induction accelerator has the merit of being electrodeless, thereby eliminating electrode erosion as a possible operational trouble. However, associated with it is a very difficult requirement on the closeness of the initial coupling between the primary coil and the secondary gas circuit. We illustrate in Figure 1 the case of a flat toroidal coil which, when pulsed, induces an oppositely directed current in the gas near the coil. Now it is evident that when the acceleration is completed and the plasma gone, the inductance seen at the coil terminals is just L_p , that of the coil alone. Hence, this becomes an upper limit on ΔL ; i.e., $\Delta L < L_p$. The initial inductance L_0 seen at the terminals when current is flowing in the gas at the beginning separation z_0 between the coil and the gas current ring must then be much less than L_p , and it is easily shown that this requirement is met by having the initial gas current flow tight against the coil, i. e.,

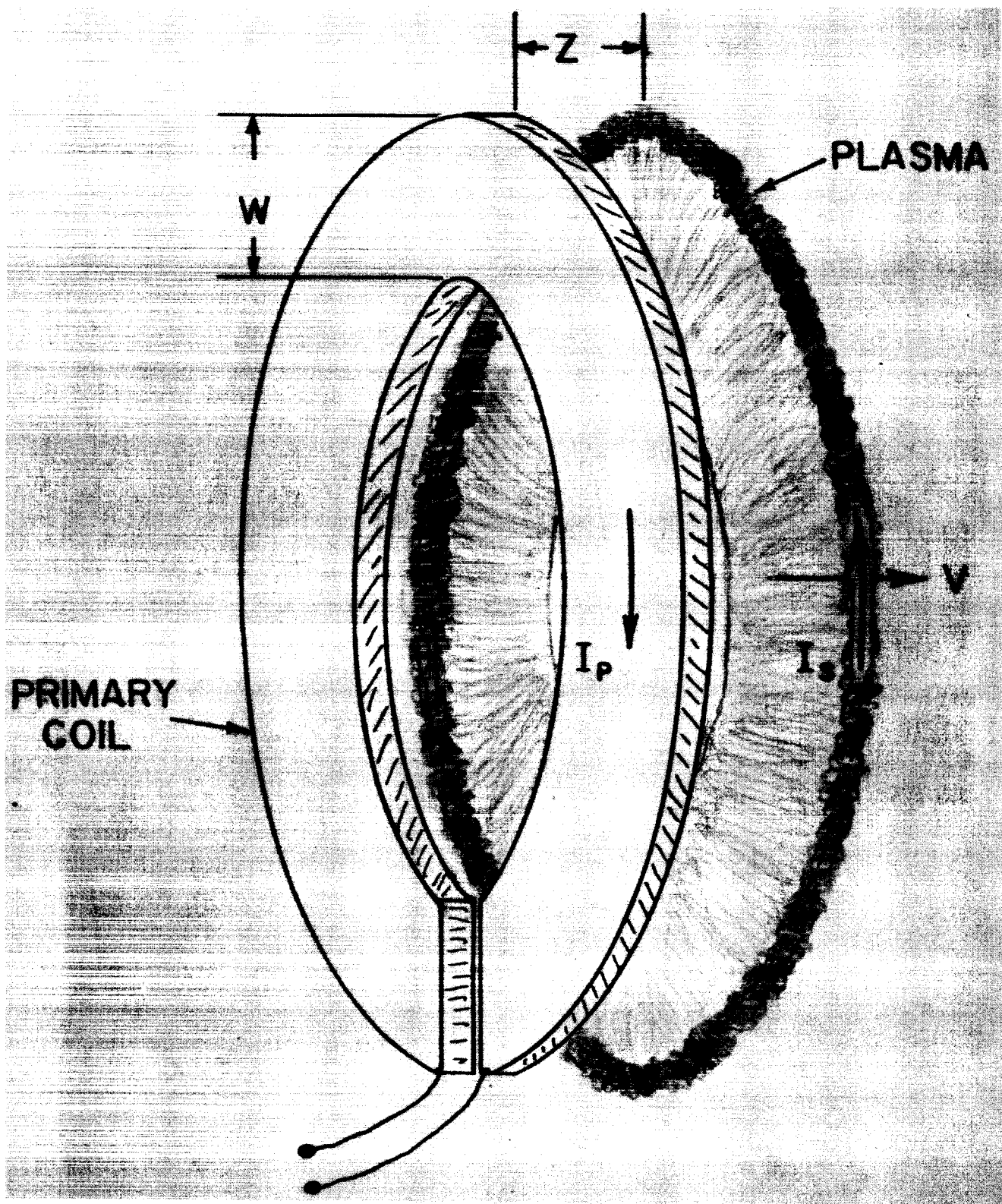


FIG. 1. SCHEMATIC OF AN INDUCTION ACCELERATOR.

$z_0 \ll w$, where w is the width of the coil. This is usually hard to achieve, since a certain thickness of insulation must be interposed between the two currents, and also because the initial gas current does not usually flow in a very thin layer. Furthermore, the two circuits are almost fully decoupled when $z = w$; hence all the energy must be delivered in a time t such that

$$t \ll \frac{w}{v},$$

where v is the velocity of the plasma. For $v = 10^7$ cm/sec, and $w = 10$ cm, we obtain $t \ll 1$ μ sec, a quite hard electrical requirement. Both of these difficulties can be alleviated, however, by going to very large w , i.e., broad coils.

The "rail gun" plasma is always tightly coupled to the energy source, since it is in series with it. This is not, of course, sufficient to assure efficient acceleration, since a large parasitic source inductance could quickly put a low upper limit on $\Delta L/L_0$; it does mean, however, that one is not forced into accomplishing the entire acceleration before the plasma has moved a small fraction of the system dimensions. Problems associated with the electrical breakdown of the propellant gas are also less difficult with a series rail gun, since if there is a formative time lag, the energy supply must simply wait until breakdown occurs. In an induction device, a delay in gas ionization results in a bypassing of the energy through the primary coil, with the associated dissipation. It is common experience in the thermonuclear research, for example, that it is extremely difficult to make fast induction accelerators break down on the first half-cycle of the oscillatory driving current.

A clear disadvantage of using a rail gun is the existence of electrodes in the plasma circuit. Since these are immersed directly in the ionized gas, they are subject to bombardment and erosion. However, it is not clear at present how rapid this erosion might be under conditions contemplated in a propulsion application. Assuming that some does occur, it is not difficult to conceive schemes for electrode replacement, periodically or even continually. A limit on erosion rate would, of course, have been exceeded when the rate of electrode material loss exceeds the rate of propellant flow.

From experiments to date, it seems that this will probably not happen.

It is important also to point out that erosion may be an equally serious problem in induction machines, but in this case, it is erosion of the insulator. The initial breakdown in these devices occurs on this surface⁽¹⁾, and always results in the appearance of spectra of insulator materials in the discharge. In the case of "Scylla", a high energy inductive pinch at the Los Alamos Scientific Laboratory, several hundred discharges caused the almost complete erosion of a 1/8" thick Al_2O_3 insulator.

An evaluation of these considerations led to the conclusion that the coaxial version of the rail-gun would be very suitable for an experimental program on MHD propulsion. It is relatively easy to construct, can be operated over a wide range of energy-source periods, and has a geometrical symmetry which makes the interpretation of electromagnetic field data simpler than in any other device. There was also available, in the case of one of the authors, (RHL) a considerable amount of experience in operating coaxial plasma accelerators for thermonuclear applications.

The coaxial configuration was also felt to be distinctly preferable to other "rail gun" configurations, since it is the only one, topologically, which is free of edges. That is, the advancing current sheet, assuming that it retains azimuthal symmetry, is a completely tight piston where in the case of parallel plates or rail pairs, one always has to deal with the leakage of propellant around the edges of the sheet, and also with gross instabilities initiated at these edges.

B. Choice of Circuit Parameters

We have seen that the efficiency of energy transfer from the storage capacitor to the plasma kinetic motion is given, in electrical circuit terms, by

$$\epsilon = \frac{\frac{1}{2} \int I^2 L \cdot dt}{W_0} ,$$

where here, $W_0 = \frac{1}{2} C V_0^2$.

Clearly, one must effect a gun design for which the total inductance increase corresponding to the removal of some large fraction of W_0 does not exceed the total available inductance of the barrel. Otherwise, the situation would exist where at the instant of plasma emergence from the barrel, most of W_0 would still be $\frac{1}{2} (CV^2 + LI^2)$, with the result that the plasma would either draw out with it a long plume of current which would accelerate mass equally in the transverse and longitudinal directions, or, if the circuit should somehow be broken, it would leave most of W_0 behind, probably to dissipate in resistive secondary breakdowns.

At the other extreme, one can conceive of the plasma slug being sufficiently heavy so that by the time the stored energy has rung down to zero in its characteristic damped oscillation, the mass has not moved far in the barrel. This usually is a case of $\Delta L/L_0 \ll 1$, and by arguments given previously, the energy transfer cannot be large.

It is easy to see that some kind of a "matching" between the electrical circuit parameters and the propellant mass or velocity must be achieved. There are several equivalent ways of stating this requirement. We may simply ask the electrical "period" \sqrt{LC} of the circuit, where L is the barrel inductance, to equal the transit time defined as $t = \frac{\ell}{v}$ where ℓ is the barrel length and v is a mean plasma velocity in the gun. Thus,

$$\sqrt{LC} = \frac{\ell}{v}.$$

If now we set $L = L' \ell$, where L' is the inductance per unit length of the gun, this reduces to

$$\ell = L' C v^2.$$

In a coaxial gun, $L' = \frac{\mu_0}{2\pi} \ln \frac{b}{a}$ where b and a are, respectively, the outer and inner barrel radii. This quantity, then cannot vary too far from $\frac{\mu_0}{2\pi}$, or 2×10^{-7} h/m. Since v itself is determined by our requirement on specific impulse, we see that ℓ and C are proportional to each other in an optimum gun.

It is of interest to note that this requirement can also be stated

as one for "impedance" matching. If we set $L = L' v$, and substitute into $\sqrt{LC} = \ell/v$, we obtain immediately

$$\dot{L} = \sqrt{\frac{L}{C}},$$

where both sides have the dimensions of an impedance. For $L' = 2 \times 10^{-7}$ h/m, and $v = 10^5$ m/sec, this impedance is

$$Z = L' v = L = 2 \times 10^{-2} \text{ ohms.}$$

From this form of the matching requirement one may observe that efficiency will be good only if all the dissipative circuit losses add up to a resistance much less than 20 milliohms.

A third, and somewhat more exact statement of this matching requirement can be obtained by writing the "magnetic gun equations". Neglecting resistance, we have

$$V_0 - \frac{1}{C} \int I dt = L \dot{I} + \dot{L} I,$$

the voltage equation, and Newton's second law

$$m \frac{d^2 z}{dt^2} = \frac{d}{dz} \left(\frac{L I^2}{2} \right) = \frac{I^2}{2} L',$$

where m is the mass of the gas slug, and z is the displacement along the barrel. We render these equations dimensionless by setting

$$i = \frac{I}{I_0},$$

where

$$I_0 = V_0 \sqrt{\frac{C}{L_0}},$$

and

$$L_0 = L' z_0.$$

Also

$$\tau = \frac{t}{t_0},$$

where

$$t_0 = \sqrt{L_0 C},$$

and

$$x = z/z_0.$$

then,

$$1 - \int i d\tau = 1 \frac{dx}{d\tau} + x \frac{di}{d\tau},$$

and

$$\frac{d^2 x}{d\tau^2} = \kappa i^2,$$

where

$$\kappa = \frac{C^2 V_0^2 L}{2mz_0}.$$

These equations may be solved numerically, with the solution being determined only by κ . L/z_0 includes whatever parasitic inductance exists in the external circuit.

Now, resistance has not been included here and so these equations are not properly useful for determinations for efficiency. However, we may impose other conditions, e.g., that at the time the mass emerges from the gun, the current shall be passing through its first zero; we then may inquire as to how much of W_0 has been transferred to the plasma at that time. We discover that this fraction is largest for κ of order unity and a barrel length large compared to z_0 . This also means, of course, that $\Delta L/L_0 \gg 1$. Aside

from efficiency, however, the principal utility of this formulation is that all the scaling relationships we need are contained in κ . If κ is such as to give optimum performance, for example, any rearrangement of C , V_0 , L' , z_0 , and m which leaves κ unaltered will also leave the matchings of "impedance" or energy the same as they were. Or, alternately, if κ appears to be incorrect, it can be adjusted in any of several ways, some of which may be much easier than others, depending upon circumstances. (A good example of this point is contained in the following work, in particular, the change from the Mk II to Mk III versions of the coaxial gun.)

Given that in an optimum design, l and C should approximately vary together we may then inquire as to what other criteria might dictate a choice of size for either or both of these parameters. It will be argued here that for separate reasons, it is desirable that both parameters be small.

Consider the capacitance first. In the application of a pulsed device to propulsion, it will be necessary to operate the gun at a repetition rate which is determined by the momentum transferred per shot and the desired thrust. The power required will be the repetition rate times the gun energy per shot. Since the system mass per unit power must be kept to as low a value as possible, it seems that one must restrict consideration to small capacitor banks run at high repetition rates.

But quite independently of firing rate, the total energy passed through the capacitor per unit time is the product of average thrust and exhaust velocity. The power dissipated in the capacitors themselves is approximately the capacitor Q divided into 2π times the total gun power, hence, for example, an engine of 1 kg thrust at 10^4 sec I_{sp} using capacitors with a Q of 30 would dissipate on the order of 200 kw as capacitor losses. Only a very large, heavy bank or an entirely novel capacitor can withstand such heating and not be destroyed quite quickly. (While one way to avoid the issue might be to settle for a few dynes thrust with conventional components, it seems that electrical propulsion does not come entirely into its own until more substantial thrust is achieved. Consequently it appears appropriate to wrestle with the components problem at this early stage.) We

have, therefore, considered the use of capacitors employing very low-loss dielectrics, and in particular, the use of vacuum. A vacuum dielectric capacitor has many attractive attributes as well as clear disadvantages. The capacitor Q is extremely high, since dielectric losses, ordinarily the principal loss in an energy-storage unit, are entirely absent. Conduction losses in the electrodes can be tolerated since there is no obvious reason that such a unit could not be operated at red heat. An occasional flash-over does not mean a ruined capacitor, and so reliability is improved. There is no dielectric mass to orbit and an infinitely good vacuum pump is always available above the atmosphere. On the other hand, the construction of such a unit is a formidable undertaking, since many thousands of square feet of plates, spaced by a very few millimeters would have to be arranged in a compact package and be sufficiently rugged to stand a flight environment. The unit would have a great deal of bulk per unit capacitance or energy, and it is likely that the advantage of having no dielectric mass at all would be more than offset by the heavier mass of plates and structures. Nevertheless, the structural problems are matters of technique rather than principle, and one can reasonably expect adequate engineering solutions in not too long a time. Therefore, it was decided to use an initial capacitance value which might be achieved by a vacuum unit. This was determined to be the order of one microfarad.

The use of a small barrel length, which as we have seen, is corollary to a low capacitance, is desirable, however, on independent grounds. First, the effect of plasma cooling to the electrodes may be made very small if the total time the plasma spends between the electrodes is very small compared to an ion transit time from one electrode to the other at thermal velocity. The actual escape of thermal energy to the walls is actually much slower than it would be in the case of free single particle motions, since collisions and, in particular, the presence of strong magnetic fields inhibit particle flow.

Secondly, it is demonstrable theoretically that as the acceleration is increased, or, rather, as the acceleration time is shortened, the formation of the most troublesome instabilities in the current layer is less advanced; i.e., the acceleration of instability growth increases less rapidly than the

acceleration of the gross plasma displacement. In accelerators of "normal" lengths, it is usually observed that the initially symmetric current distribution tends to develop unevenness in the azimuthal direction which in the end results in all the current flowing in a narrow rod, or "pinch", at one side of the tube. In this case, there is no longer an efficient sweeping up of the injected propellant, and the mass utilization becomes very poor. It has been found in the work to be described that these instabilities have indeed been greatly inhibited.

The various equations of motion and scaling laws given above are at best, however, only a rough design guide. The reasons are twofold. First, they are derived on the assumption that the plasma slug is a compact entity which has no resistance, either in bulk or as drag on the electrodes. No current is supposed to flow anywhere except through the narrow slug. As will be seen, this assumption is at best only approximated and in many instances is not even a qualitative description of how the system behaves. In spite of this, many of the scaling laws still apply.

Secondly, the use of a scaling relationship between the several parameters characterizing a system presupposes that one can vary them independently, except for the given constraint which in our case is $\kappa (C, V_0, L', m, z_0) = 1$. This is not the case in the present work, however. The mode of operation we have selected makes the slug mass m critically dependent on V_0 and L' , and to some extent on C and z_0 . This deprives one of complete freedom in use of the $\kappa = 1$ equation, and probably means that another and more useful scaling law could be written if one knew in enough detail the dependence of gas breakdown on voltage, electrode spacing, and propellant species.

C. Mode of Gun Operation

The same concept of operation is common to all the devices described in this report. An ideal operating sequence would be the following:

1. The storage capacitor, which is connected directly to the electrodes, (there are no switches in the circuit), is charged to V_0 .
2. The valve controlling the propellant gas flow is opened and left open.

3. When the gas density immediately over the gas ports in the center electrode has risen to the appropriate value, a breakdown occurs, and the normal acceleration cycle proceeds.

4. After the shot, the inter-electrode gas pressure again rises, and the capacitor re-charges. The latter is adjusted to occur much more rapidly than the gas influx, so when the propellant pressure once again reaches the breakdown value, the capacitor is fully charged, and the whole process repeats.

This operating concept has the merit of extreme simplicity, since neither high-current switching nor oscillating gas valves need be employed, and system reliability would consequently be improved. However, there exist possible technical problems with the idea which may, in the worst case make it unfeasible. In particular, the full injected gas load is not ejected during a single shot of the gun. Breakdown usually occurs near the peak of the injected pressure distribution, and since this distribution (in z) is approximately a symmetrical Gaussian centered over the gas ports, one might, in the case of a simple current-sheet acceleration expect up to half of the gas to be left behind. One could argue that this left-over gas would simply add to the new influx for the next shot; however, the shape of the gas distribution, just prior to breakdown, is important in that the pressure should be low near the rear insulator in order that the discharge should not occur there. With a shot-to-shot accumulation of leftover gas, however, it seems that the pressure at the insulator could easily rise to the breakdown level, thus resulting in undesirable insulator erosion. The actual evaluation of this problem will have to await high repetition-rate experiments which have not yet been accomplished.

The repetition rate which would arise naturally from this free-running mode is determined by the time required for the gas filling. Depending upon the propellant species used, the internal delay might be a few hundred microseconds to somewhat more than a millisecond. Slower firing rates, say one hundred shots per second, will almost surely necessitate the use of an oscillating gas valve rather than steady flow.

D. Experimental Program

With the general principles outlined above as a guide to the general design of an accelerator we have established an experimental program directed toward determining, in as direct and unambiguous a way as possible, whether the coaxial gun concept in this form is feasible for propulsion.

Our program has dealt with two broad areas: 1) the physics of the acceleration process in a coaxial gun, especially those phenomena which influence efficiency, and 2) the engineering feasibility of the free gas-flow, high repetition rate mode of operation discussed previously.

In general, we have tended to give priority to the physical measurements of plasma phenomena in the gun. The reason is simply that until we understand the acceleration process in detail, there are no clear guideposts for optimization of the design. Conversely, if it can be demonstrated, using the single-shot operation we employ in these measurements, that plasma acceleration in this device is intrinsically inefficient and unsuitable for propulsion, there will be no point at all in making the gun fire at a fast rate. However, preparations for fast firing have gone forward.

The experiments undertaken in the course of this work have been done on a series of coaxial guns which successively incorporate parameter changes dictated by the experimental results. We designate these as Mark I through Mark IV. We will discuss their characteristic parameters and experimental behavior chronologically and defer a description of mechanical details to appendices at the end of this report.

The principal diagnostic tools employed in this work have been magnetic and electric probes. Each type of probe is a powerful instrument, but in combination, they allow the inference of a very wide range of plasma parameters, and are superior, for our purposes, to any other available diagnostic technique. We will first discuss their use in some detail.

E. Magnetic Probes

The magnetic probe technique has been employed successfully in experi-

mental plasma physics for several years⁽²⁾. It simply consists of inserting a small coil, suitably protected by an insulating jacket, into the plasma. The coil output is passed through an integrating circuit, (since its direct output is proportional to $\partial B/\partial t$) and the integrator output is displayed on an oscilloscope. The initial rise of current in the pulsed plasma device under study is used to trigger the oscilloscope, which then displays a graph of $B(t)$ at the probe position. If the device is sufficiently reproducible from shot to shot, (as may be determined by photographically superposing traces taken at one position) the field may be mapped by moving the probe to various positions and repeating the procedure. Having, at the end of an experiment, a set of photographs of $B(t)$ traces at various positions, one may then select a certain instant of time, common to all the traces, and plot $B(\vec{r})$ at that time. In the following descriptions of experiments, we display several such maps of B . It is usual that only one, or at most two, components of B are present in the apparatus under study, and usually there is sufficient geometrical symmetry in the device to allow a fairly simple application of the Maxwell equation

$$\text{curl } \frac{\vec{B}}{\mu_0} = \vec{J}, \text{ (mks)}$$

(where μ_0 , as always, is the permittivity of free space) and hence, a determination of the current density distribution. For example, in our coaxial gun, in the absence of instability, only B_θ is present, and the above equation reduces to $\mu_0 j_r = \partial B_\theta / \partial z$. The Lorentz force on the plasma along the barrel is then just

$$(\vec{f})_z = (\vec{j} \times \vec{B})_z = \frac{B_\theta}{\mu_0} \frac{\partial B_\theta}{\partial z} = \frac{\partial}{\partial z} \left(\frac{B_\theta^2}{2\mu_0} \right).$$

There are some legitimate objections which can be raised to the use of magnetic probes in the manner described above. The most fundamental is that there exists a hazard of altering the properties of a plasma by the very act of thrusting a material object into it. A certain volume immediately around the probe jacket is certainly cooled to some extent, and as a conse-

quence becomes more resistive. To this objection one can only bring the results of considerable experience and experiment on this point, together with a semi-qualitative justification of the technique in certain temperature and density regimes. We first observe that in a system characterized by broad and continuous current distributions, the magnetic field at any point is the vector sum of contributions from current elements throughout the system. Stated in other terms, the complete removal of the current density in a small region will not, in general, seriously change the local magnetic field; this is the very argument that applies to a magnetic probe. It is not valid, however, in the case of nearly discontinuous field distributions where the sharper features of the field pattern are necessarily produced by local currents. That is to say, some spatial resolution will be lost; it is found experimentally, however, that for plasma conditions we encounter in this work, this loss is negligible. While the above argument may be quite valid, we still are in trouble at the conduction "hole" bored by the probe is too large, in particular, if it is any substantial fraction of the system dimensions. The size of this perturbed region will depend upon plasma density and temperature, and will be largest for hot, low density plasmas. We resort again to a sufficiency argument on this point: if one can actually observe, by means of the probe, structural features of the field which are adequately small, this worry is automatically disposed of. We have, indeed, observed large field changes over distances less than twice the diameter of the probe jacket, which indicates amply small perturbation.

Another problem, in principle, in the use of jacketed probes, is that for a plasma of sufficiently good conductivity, there should be a delay in the flow of field lines out of the near plasma region and into the probe, corresponding to ordinary field diffusion times through a conductor. This delay would appear as both a delay and an attenuation on the signal read out by the probe. One is then in the dilemma of desiring that the conductivity of the plasma near the probe be neither too high nor too low - at least, not low by reason of cooling to the probe jacket. Fortunately, there are excellent operational checks on the existence of any attenuation or delay. In a coaxial gun, where under certain conditions, the current flows in a thin, azimuthally symmetric sheet, the instant of crossing a

certain point in the barrel by the moving current layer may be observed with electric as well as magnetic probes. In a situation quite similar to that in the present work, these two indications of sheet arrival were simultaneous to within the limits of detectability, indicating that any B-probe delay was negligible. In the same experiment the value of B_θ measured behind the current sheet was used to compute a total current, and this agreed well with an independent external current measurement. Similar verification experiments have been performed in pinched discharge devices, and to our knowledge, no instance of delay or attenuation has been observed. One may argue, in a semi-quantitative way, that this result should perhaps be expected. If we compute an approximate value for the conduction skin depth δ using the one-dimensional expression

$$\delta^2 = \frac{\rho t}{\mu_0} \text{ (mks),}$$

where we use the approximate Spitzer relation⁽³⁾ for resistivity

$$\rho = 3 \times 10^{-8} T_{\text{kev}}^{-3/2} \text{ ohm-m,}$$

and also assume a 10 e.v. plasma temperature, we get a skin depth of about 2 millimeters in $t = 10^{-7}$ sec. Since our probe radii are just this size, we see that an adequate rate of flux flow into the probe interior may reasonably be achieved. We have inserted a rather strong assumption on plasma temperature here, but when this device is compared, both in configuration and gas species, to such devices as deuterium pinches whose temperatures in general vary from 20 to 40 e.v., it seems certain that the heavy propellants used in these guns are not hotter than 10 e.v.

F. Electric Probes

The classical mode of electric probe operation is that attributed to Langmuir⁽⁴⁾. An insulated wire having an exposed tip is inserted into the plasma, and is biased at various voltages with respect to some refer-

ence point in the system, usually an electrode. The currents drawn by the probe for various voltages are plotted as a "probe characteristic" whose features are interpreted in terms of plasma potential, ion and electron densities and plasma temperature. Such a procedure is only valid for certain "pure" cases, however. The plasma must be in thermal equilibrium and free of magnetic fields, and the probe must be of a simple configuration, i.e., a plane, cylinder, or sphere.

In the case of the plasmas produced in our experiments, the Langmuir technique is ruled out on several grounds. A strong magnetic field permeates the system, thermal equilibrium is probably not even approximately attained, and in particular, the ion and electron densities are so high that destructive currents would be drawn to the probe if the bias potential were moved appreciably away from the "floating" value. Floating potential on an electric probe is the potential at which its current is zero, i.e., when an equal flux of ions and electrons are reaching the exposed tip. Since the flux of electrons to any open element of area is far higher than that of the ions, floating potential can only be at a value sufficiently negative with respect to the plasma potential to repel almost all the electrons. This will generally be a value of about $-kT_e/e$ (where k = Boltzman's constant, T_e = electron temperature, e = electronic charge.)

In our application, the probes are used only to determine a value of local floating potential. This determination places no demands upon the plasma in regard to accurate thermal equilibrium, or even magnetic field, since the value kT_e/e for the difference between plasma and floating potentials will be maintained whenever the electron flux is substantially larger than ion flux in the plasma, even though it may be much less than it would have been in a field-free, equilibrium plasma. Furthermore, even if the two probes have greatly different collection areas, the kT_e/e difference will be unaffected, since no current is being drawn from either. While any knowledge of plasma potential depends on an independent measure of kT , we may determine plasma potential differences between neighboring points (of similar kT) by simply noting the differences between the voltages on two probes⁽⁵⁾.

This, then, allows a determination of the average E field along a line connecting the tips.

In practice, we have employed a double probe consisting of a co-axial line whose inner and outer conductors are exposed to the plasma, at points separated by one cm along the common axis. The two outputs are fed through a pulse transformer to an oscilloscope, and the data are recorded in the same manner as described for magnetic probes. Details of construction of the probe and transformer are given in Appendices II, III, and Figures 32 and 33.

The utility of E-field determinations in this work can be seen by a consideration of the microscopic processes involved in the acceleration of a plasma by Lorentz forces. When the ionized gas is viewed simply as a fluid conductor, the statement that $\vec{f} = \vec{j} \times \vec{B}$ suffices, together with the value of local density, to determine the acceleration of a volume element. However, in a real plasma, the conduction current is carried almost entirely by the electrons, and the Lorentz force is applied to them alone. The electrons tend to move ahead of the ions as a result of this preferential acceleration and in so doing, set up a space-charge separation field which in the cylindrical coordinates of our guns is E_z . This E_z field, then, acts on the ions and accelerates them such that in a gross sense, there is never a large physical separation of positive and negative charges.

Since the ions contain almost the entire plasma mass, and the electrons carry essentially all the current, one may simply equate the electrostatic force per unit volume on the ions to $\vec{j} \times \vec{B}$. In cgs units, this becomes

$$n_1 e \vec{E} = \frac{\vec{j} \times \vec{B}}{c},$$

where n_1 = ion density; or

$$n_1 e E_z = \frac{B_\theta}{4\pi} \frac{\partial B_\theta}{\partial z}.$$

Now, this allows, in principle, a means of determining the distri-

bution of ion densities, since our two kinds of probes give E_z , B_θ , and $\partial B_\theta / \partial z$ explicitly. The data shown later in this report include such calculations.

Another direct use which can be made of the E_z distribution is the estimation of the directed velocity of ions after the acceleration cycle is complete. Since, for present purposes, we assume that momentum transfer to ions is entirely through the electric field, we simply write

$$m_i \Delta v = \int e E_z dt .$$

Now, since the output of the electric probe is proportional to the average $E_z(t)$ between tips, we need only to integrate the oscilloscope readout of E_z to get a measure of Δv . However, the procedure is, in general, not as simple as integrating a single trace from one position of the E probe, since during its acceleration, the ion moves from one probe position to another, and we must follow the ion in measuring the momentum transfer. This makes necessary a piecemeal integration, where $E_z(t)$ at one position is integrated only up to such a time where the ion would have crossed over into the domain of the next E_z trace in the mapping. The procedure is then continued in this fashion until E_z at the ion goes to zero. Examples of this type of velocity determination are given in the following descriptions of experiments.

G. Experimental Devices and Results

1. Mark I

The first experiments performed under this contract were done on an accelerator designated Mark I. The device is shown in the photograph of Figure 2, and the pertinent electrode dimensions and gas feed position are listed in Table 1, page 45. A magnetically operated gas valve was located inside the central electrode, and since this electrode was mounted directly on the high voltage terminal of the single 1.6 μ fd, 25 kv. storage capacitor, the pulsing circuits for the valve were all battery operated and isolated from ground.

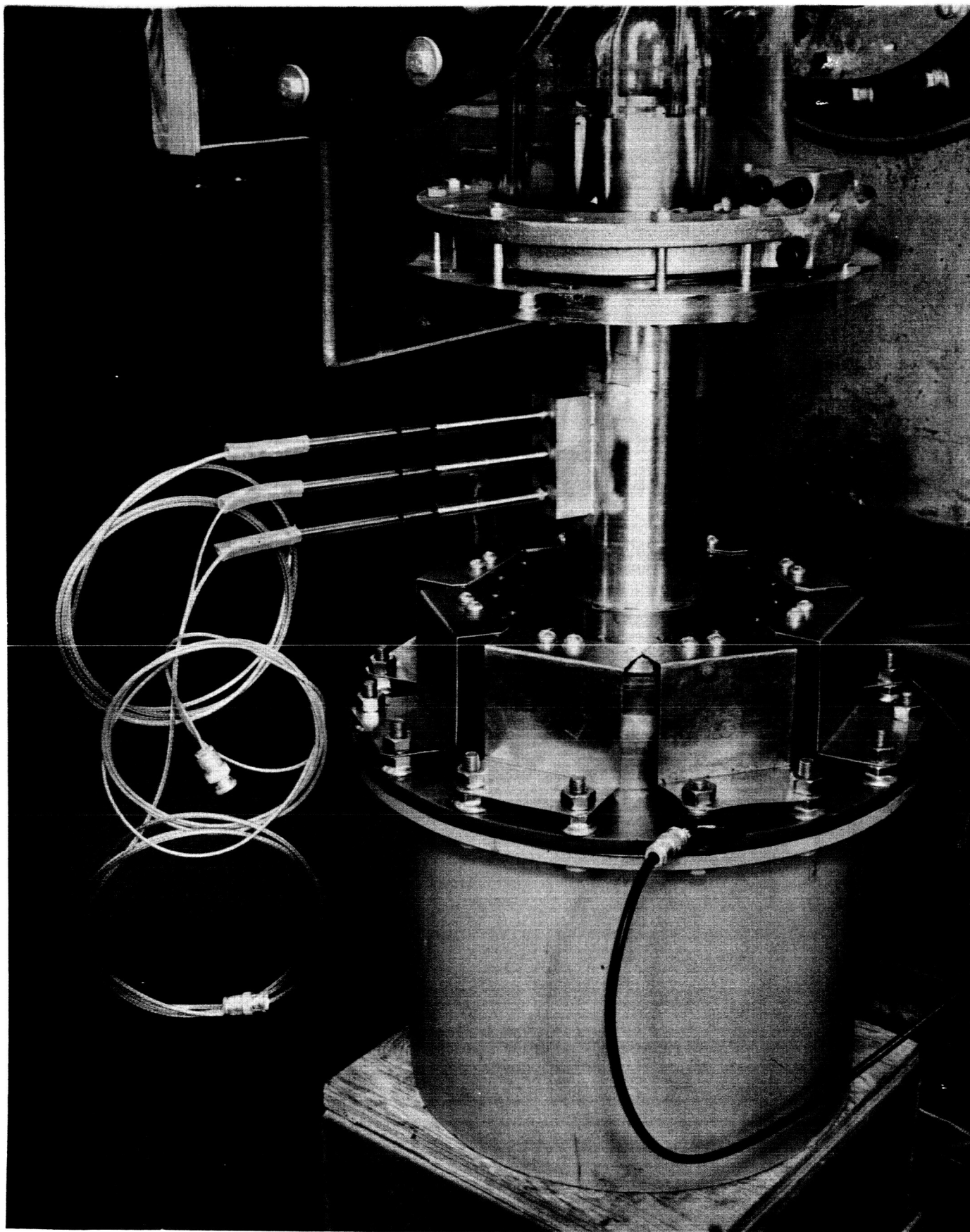


FIG. 2. MARK I COAXIAL GUN

The center electrode was the cathode in this and all the following experiments. Some brief running was done at the opposite polarity, and it appeared that the central cathode gave the least erratic operation; however, no systematic study of this effect was made during the period of this report.

The large 3' x 3' x 4' vacuum tank provided as a free expansion volume for the expelled gas from the gun was not actually employed in these experiments for the reason that it did not allow easy access to the gun muzzle for the use of probes. Instead, a cross of standard 6" glass pipe was attached to the tank port, and the gun inserted into one of the transverse arms. The opposite arm was then used to mount probe feed-throughs.

It was recognized at the outset that the external parasitic inductance of this gun was too large for efficient operation in terms of the $\Delta L/L_0$ criterion. Nevertheless, it was felt that such an accelerator would be very important to our program in many other ways. First, for studies of the acceleration process, the external inductance is not of fundamental importance. Furthermore, this initial phase of the program would have as its main function the proving out of various experimental and operational techniques, and here, again, the inductance issue is not important.

The electrical schematic of Figure 3, which applies in particular to the Mk II through Mk IV guns, is also applicable here, except that as stated before, the gas pulser was isolated from ground, battery operated, and fired through an isolating H.V. pulse transformer. After each shot, the capacitor was re-charged through the indicated 2 megohm resistor, and this, together with the time required to pump the system free of the injected gas, limited the shot repetition rate to two, or at most three, per minute. A solenoid-operated needle valve was used to admit the gas. Its driving circuit is shown in Figure 4. While the applied pulse pulled the needle to an effectively full-open position in probably less than a millisecond, the inertia of the solenoid core held it open for a substantially longer time, such that even after the shot, a great deal of gas entered the system. This open time was a sensitive function of the

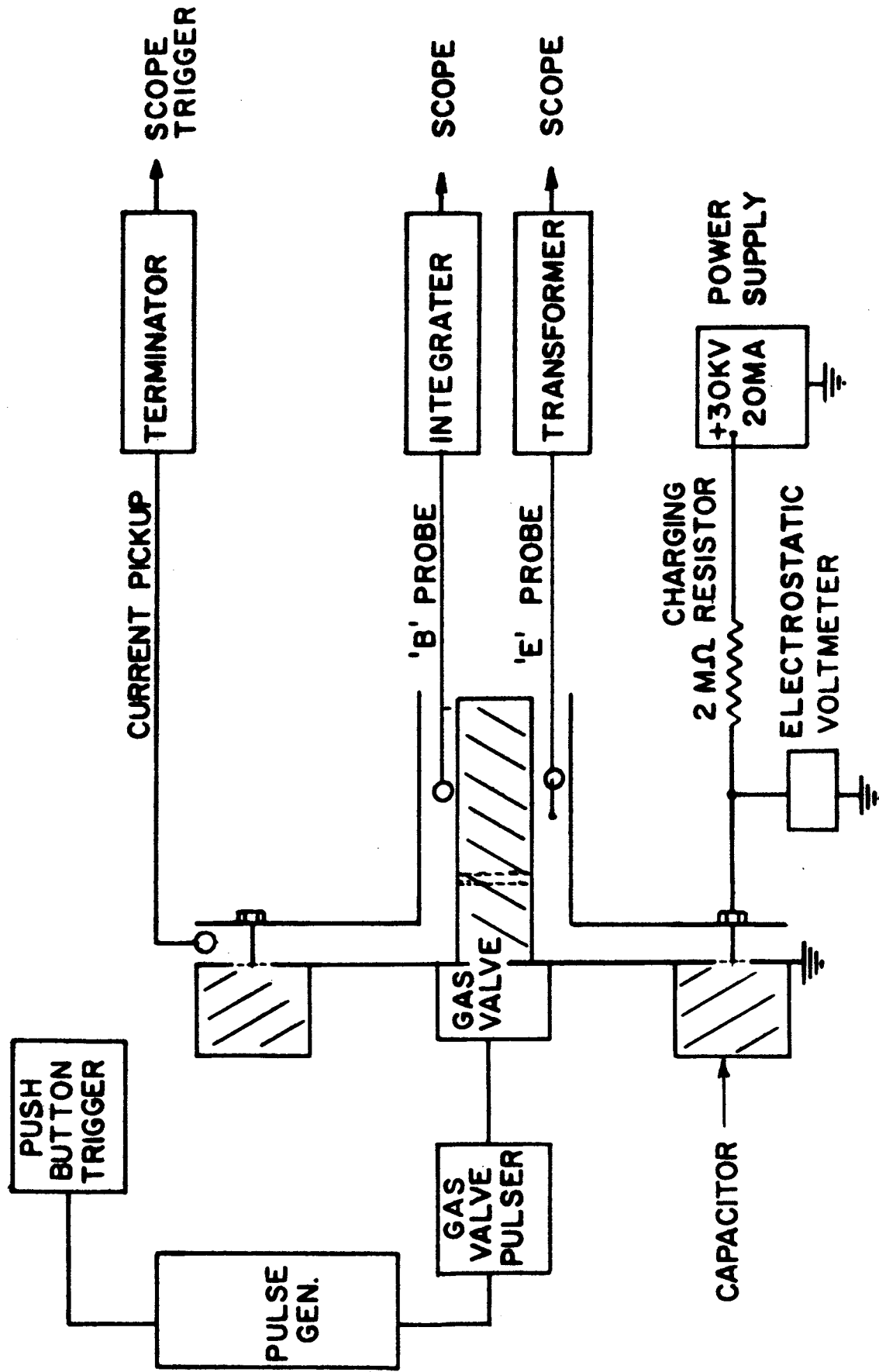


FIGURE 3. THE ELECTRICAL SYSTEM FOR THE MARK II, III, IV GUNS. THE MARK I ARRANGEMENT WAS SIMILAR EXCEPT FOR THE CAPACITOR ASSEMBLY (SEE FIGURE 2).

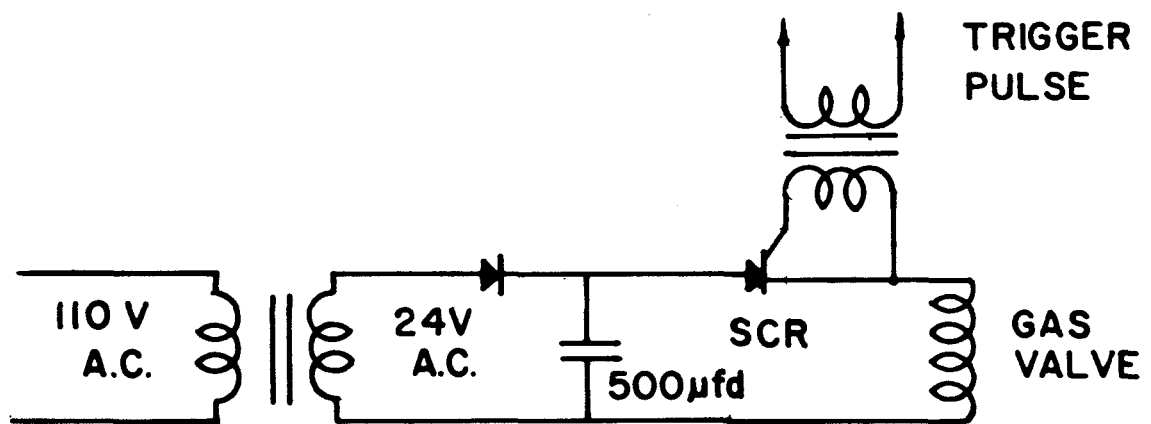


FIG. 4. GAS VALVE PULSING CIRCUIT

energy fired into the solenoid by the pulser, and the excess flow was also highly dependent of the size of the hole opened by the needle. These were all varied at different times during the experiments in an effort to develop a reliable and leak-free valve design. The best combination of an all-metal valve proved to be a polished drill-rod needle and an aluminum seat, but the reliability was not good enough, and the final solution was to put a miniature O-ring around the needle tip, as shown in Figure 5.

Since the only attribute of the valve which is important for single shot operation is that it opens quickly enough, the problem of the excess flow was ignored in these experiments.

Early operation of Mk I was involved with finding combinations of gas pressure, voltage, and valve design which would produce a discharge showing evidence of motion down the barrel. For this program, magnetic probes were used alone to observe the time dependence of B_θ distributions in the gun. The very first attempts were unsuccessful since the discharge current density peaked at the rear insulator, and remained there. The trouble appeared to be that the gas influx was too slow, with the result that by the time the pressure had risen to a breakdown level, it had distributed itself broadly throughout the tube, and onto the insulator, where the discharge initiated. An increase in gas flow rate had the effect of moving the initial current flow up to the gas ports, and the acceleration of the current layer then appeared "normal".

In all this initial program, the propellant employed was argon. The choice of gas was made on the basis of its ease of procurement and handling, as well as its advantage from the point of view of ionization loss per unit mass-flow from the gun. Clearly, at the same exit velocity, the ratio of ionization energy (a loss, in terms of efficiency) to the translational kinetic energy of the ion drops with increasing ion mass.

A fairly extensive program was necessary in order to put the E-probe into operation. While the principle of operation, which has been described before, is fairly simple, there are difficult technical problems involved. These are almost all associated with the fact that the difference voltage

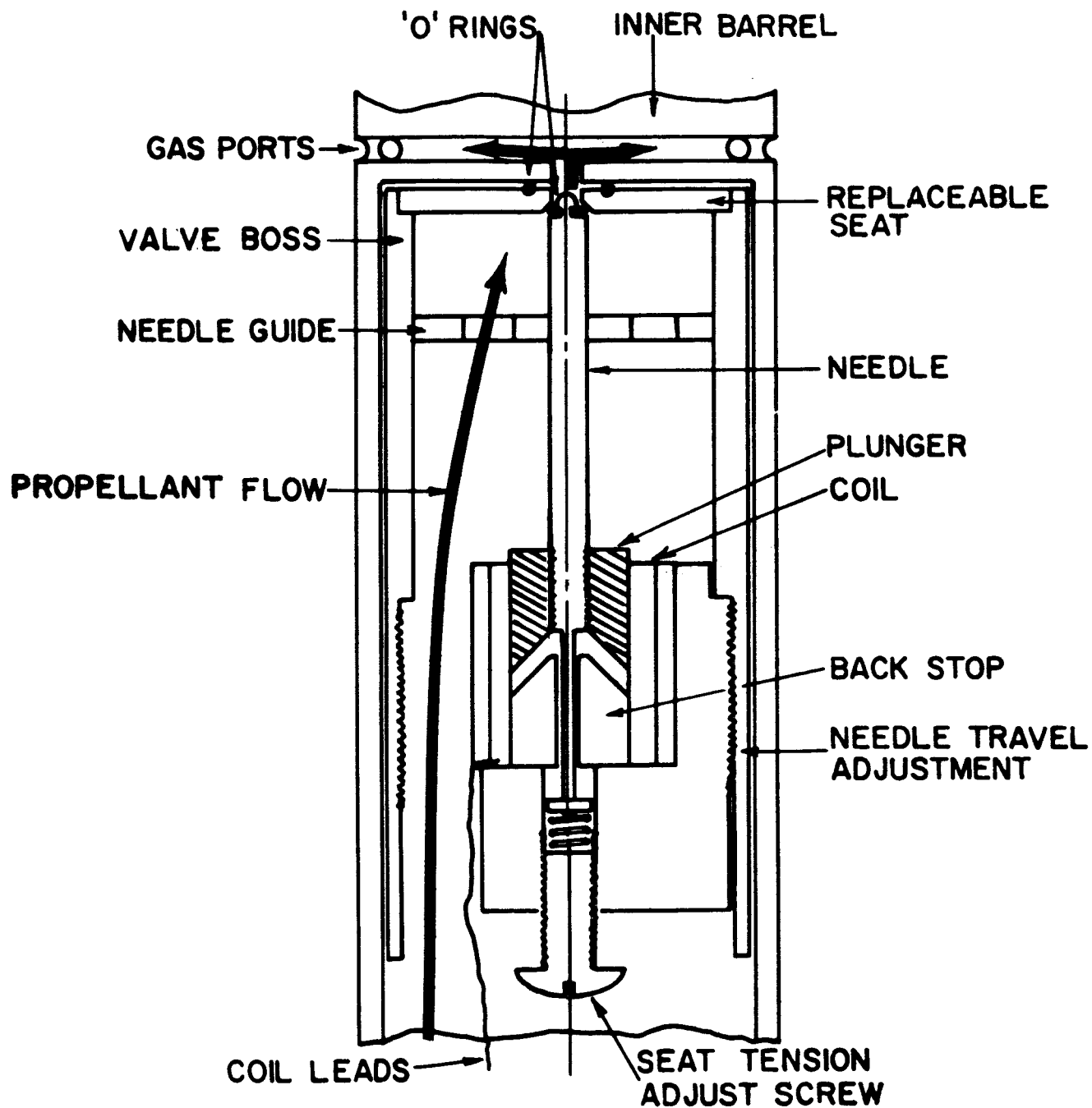


FIG. 5. CROSS-SECTION OF THE GAS VALVE

between the two probe tips is less by about two orders of magnitude than the "common mode" signal; i.e., we typically obtain a hundred volts difference between two ten kilovolt signals. The common-mode rejection in the differential circuit should then be at least a factor of 10^3 and preferably higher. In the Mk I experiments, each of the probes was brought to an external 100:1 resistive divider, and the outputs of these were sent to the two sides of a Tektronix type G differential preamplifier on a type 555 oscilloscope. It was found necessary to go to rather extreme lengths in balancing the two sides of the system in order that the common-mode rejection for the higher frequencies would be adequate. All leads had to be cut to exactly equal lengths; the dividers had not only to have the same division ratio but had to be physically identical to the extent that a small loop in a connection in one had to be duplicated in the other. The two dividers were mounted together and had to be located in a position carefully selected to minimize the difference signal resulting from their acting together as a loop, and picking up transient magnetic fields from the gun. The preamplifier itself had to be re-balanced on each of the gain ranges employed in the experiment. After considerable attention to details of this sort, the behavior of the probe was made adequate for our purposes, although there was some undesirable feed-through at the highest frequencies.

The concept of using E and B measurements together to determine ion densities and ion momentum transfer evolved during the course of this work, and as far as we know, it had never been attempted previously. The scheme seemed to be of the greatest importance at this point, and accordingly, the majority of the ensuing Mk I experiments dealt with just such determinations.

In obtaining a complete set of data suitable for finding $n_1(z, t)$, it is necessary that the system operate over a large number of shots with very good stability. The effect of such a constraint on most systems such as this, where many components are in the process of development, is to reduce the probability of success on any given run to much less than one. That is, it was typical here to have runs interrupted by failures of gun insulation, gas valve, probes, voltage supply or even the oscilloscope. However, patience was rewarded, and some excellent sets of data were obtained.

Figure 6 through 8 are plots of B_θ , E_z , and n_1 for various times subsequent to the first current rise in the gun. The operating conditions were:

Voltage	15.6 kv
Propellant	Argon
Pressure behind gas valve	170 mm Hg
E_z probe tip spacing	6 mm

Figure 9 is a set of three corresponding oscilloscope records of $B_\theta(t)$ and $E_z(t)$ at three axial positions; all were taken at a radial position halfway between the electrodes. The propagation of the current layer down the barrel is evident.

Several comments on these data are in order. First, the spatial distribution of E_z , especially for the $0.4 \mu\text{sec}$ time, appears strange at first glance, since it has a pronounced dip just where the B_θ curve is steepest, or equivalently, where j_r is peaked. However, the strangeness disappears when one calculates n_1 , since we obtain from these curves a simple peaked n_1 curve which duplicates almost exactly the distribution of j_r in z . This would be the natural consequence of a current-dependent ionization fraction, i.e., a situation where the current, as an ionizing agent, competes with some rapid recombination process. We see that this peaked ionization distribution moves toward the gun muzzle at the velocity of the current layer, ($\sim 1.5 \times 10^7 \text{ cm/sec}$) suggesting, alternatively to the ionization-recombination picture given above that a group of ions is actually being carried along by the current at this speed. A choice between these two interpretations is quickly made, however, when we calculate Δv_1 through integrating $E_z(t)$, as explained previously. We find that the largest Δv_1 that can be obtained for any starting point along the tube is about $1.5 \times 10^6 \text{ cm/sec}$, or a full factor of 10 less than the speed of the distribution! We can also rule out the larger velocity for the mass on quite independent grounds. If we use the values of n_1 given in Figure 8, and calculate the total plasma kinetic energy at $v = 1.5 \times 10^7$ we obtain approximately the whole initial capacitor energy;

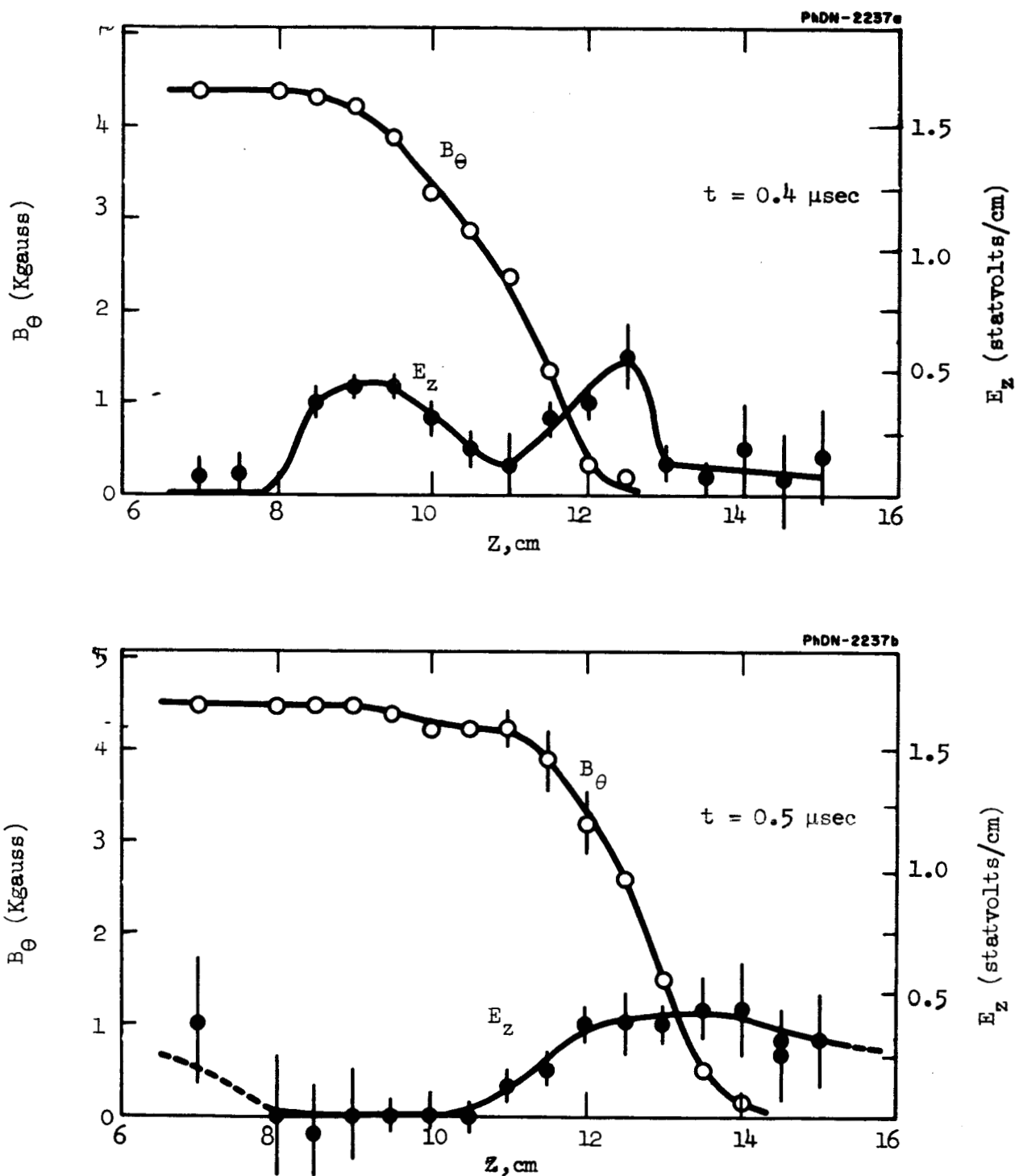


FIGURE 6. DISTRIBUTION OF B_θ , E_z , FOR THE MARK I GUN. THE GAS PORTS ARE AT $z = 10.5$ cms. TIME $t = 0$ CORRESPONDS TO THE START OF THE CURRENT RISE. THE ERRORS REPRESENT THE SPREAD IN THE DATA.

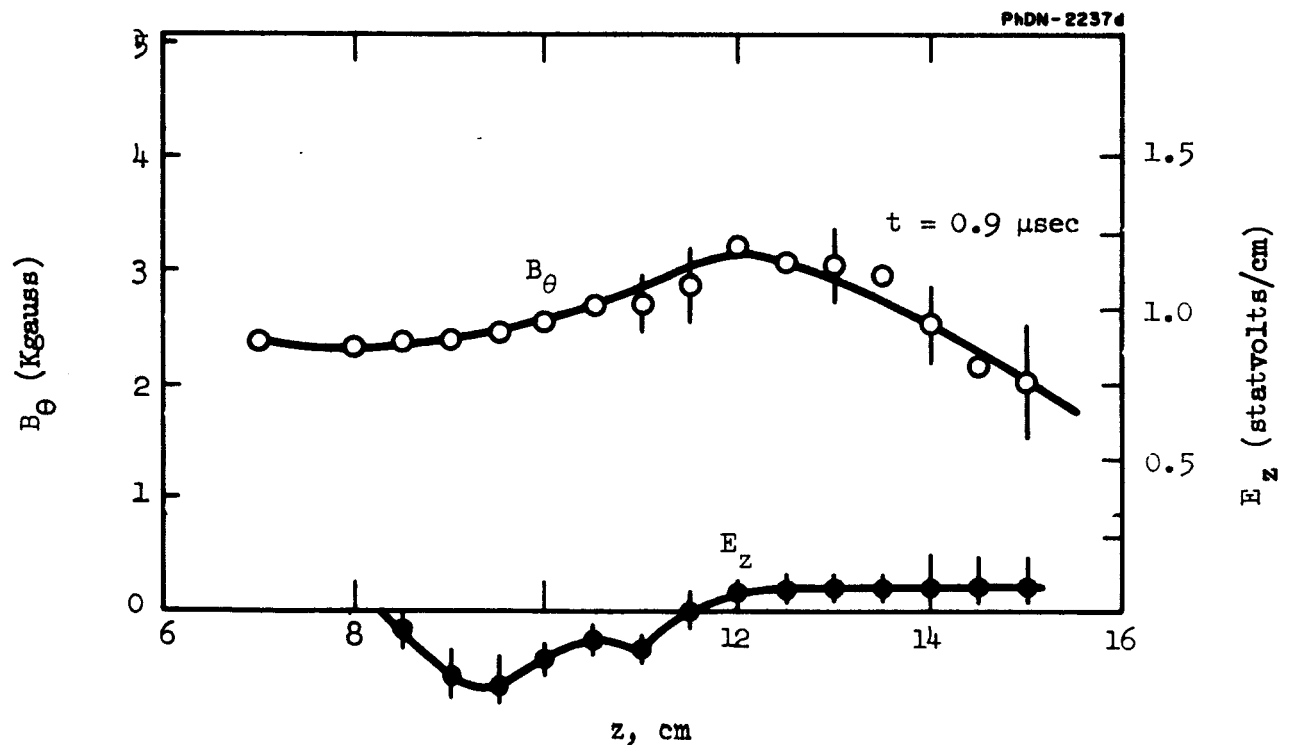
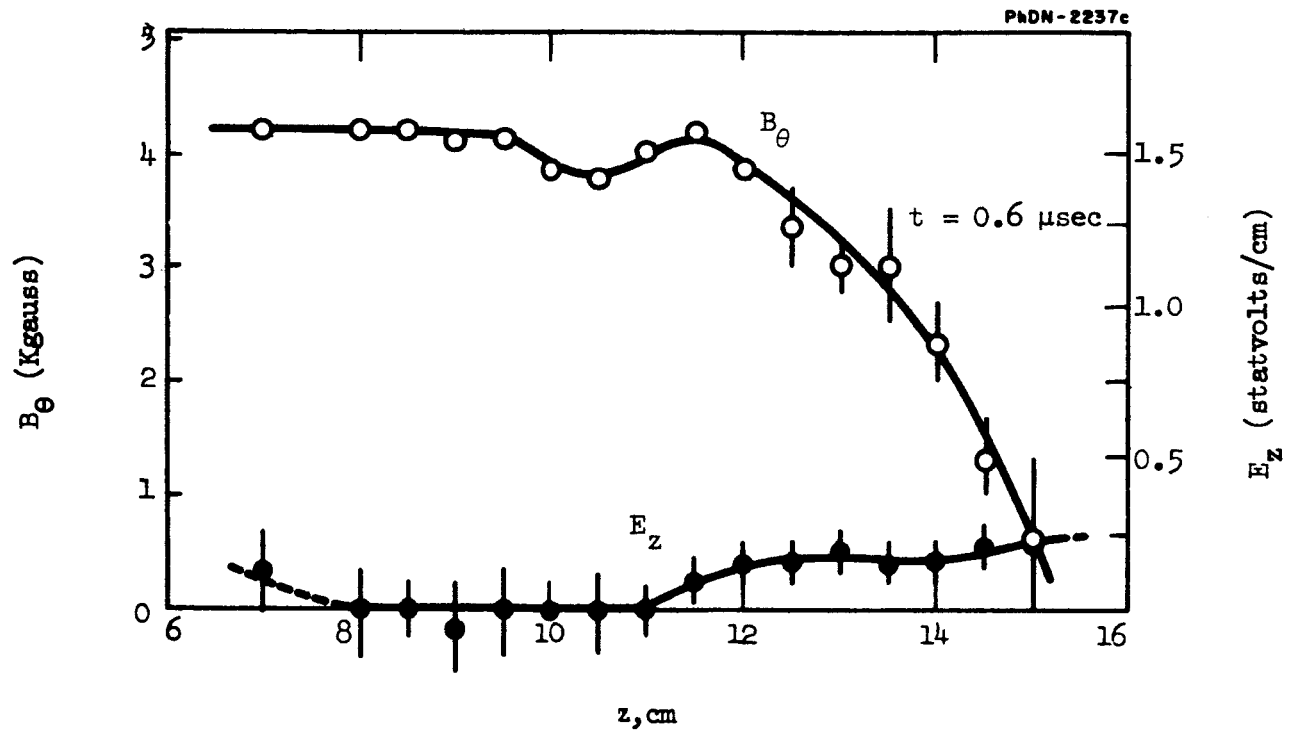


FIGURE 7. DISTRIBUTION OF B_θ , E_z , FOR THE MARK I GUN. THE GAS PORTS ARE AT $z = 10.5$ cms. TIME $t = 0$ CORRESPONDS TO THE START OF THE CURRENT RISE. THE ERRORS REPRESENT THE SPREAD IN THE DATA.

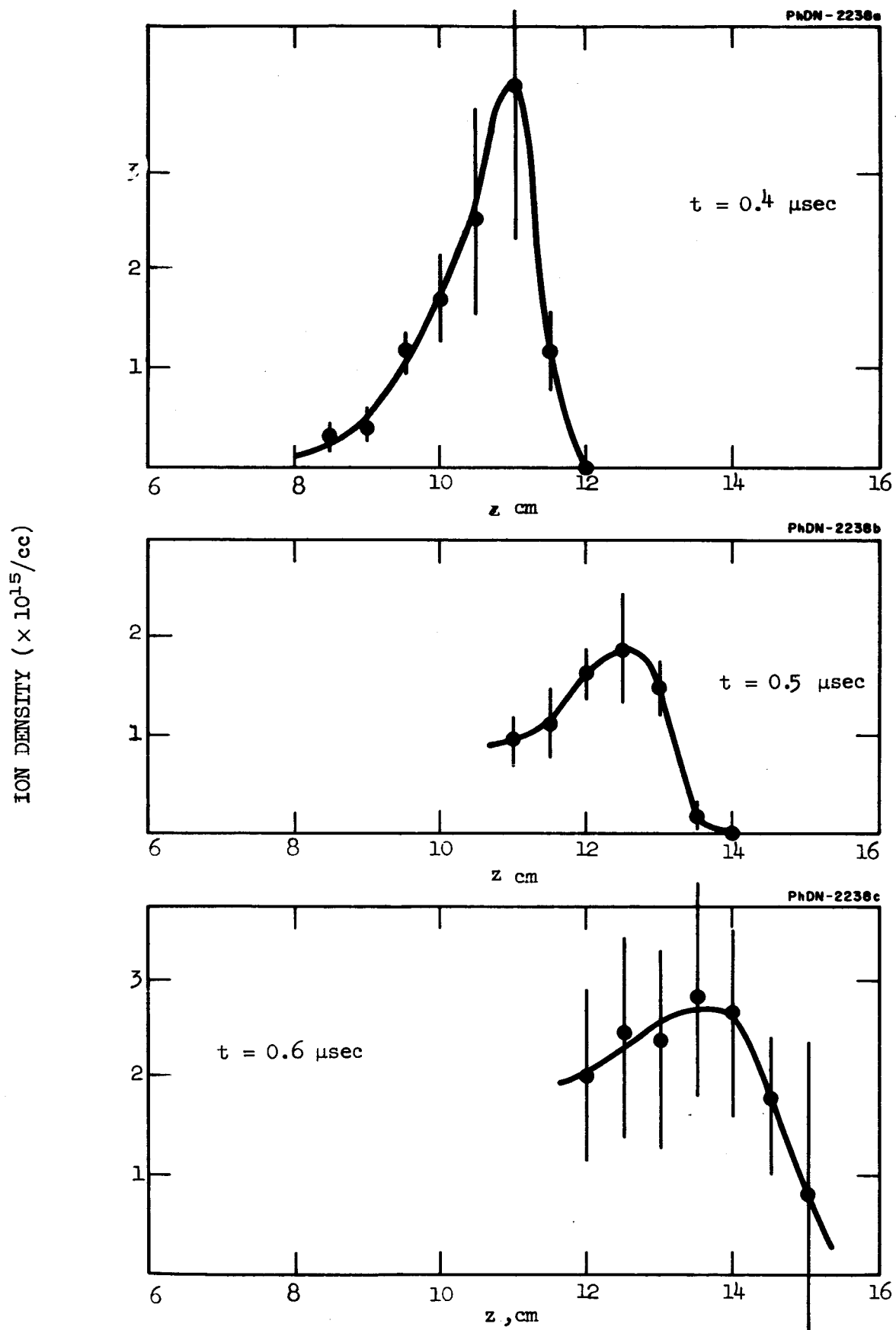
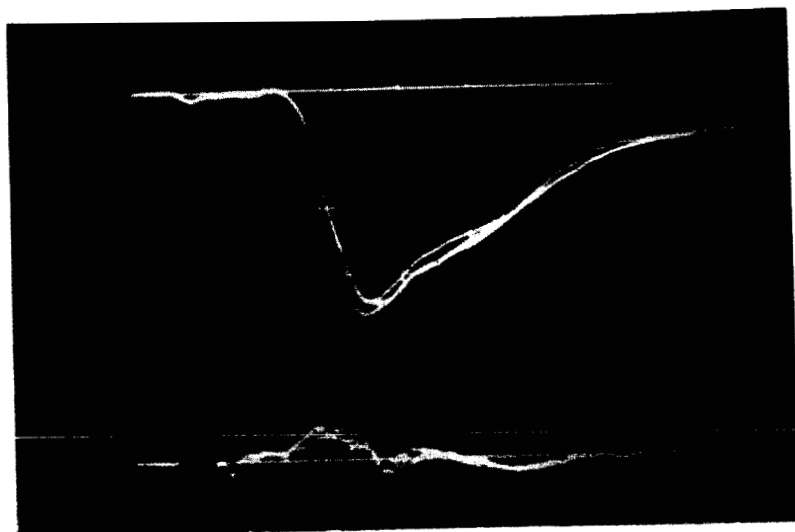
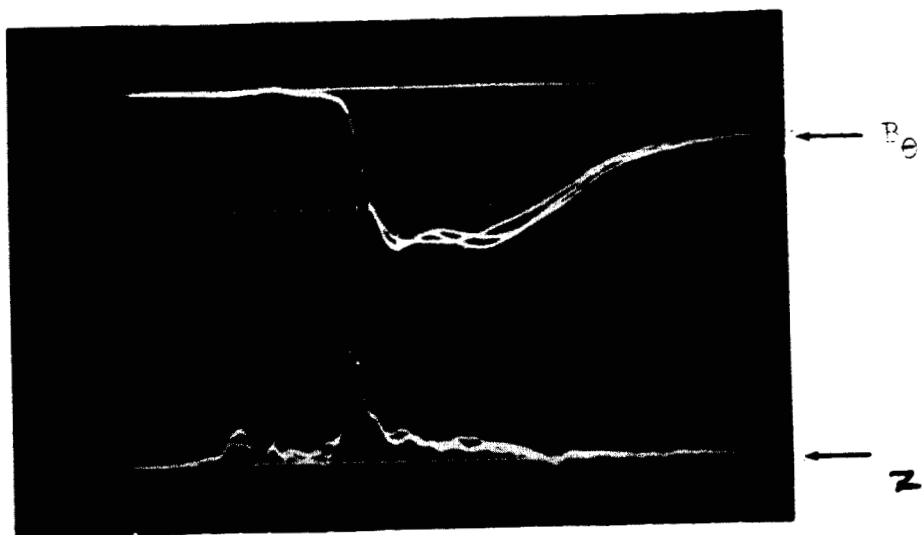
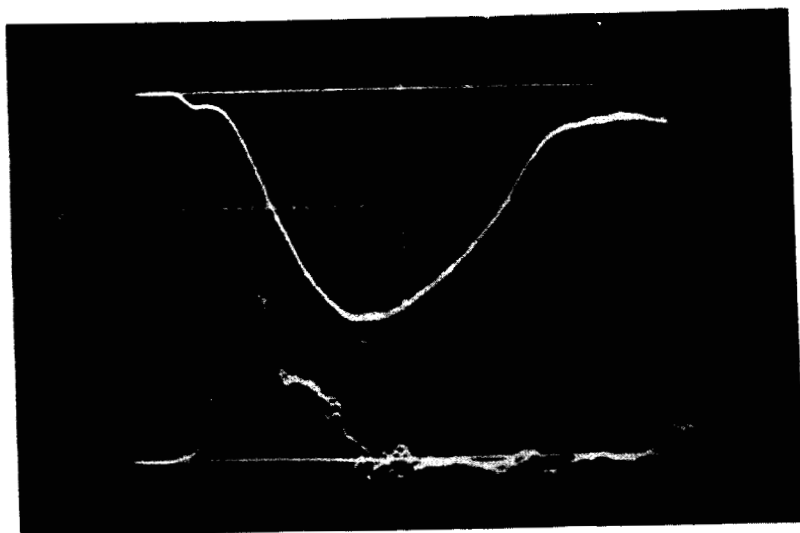


FIGURE 8. ION DENSITY DISTRIBUTIONS CALCULATED FROM THE DATA SHOWN IN FIGURES 6 AND 7.



$Z = 10.5 \text{ cm}$



$Z = 8.5 \text{ cm}$

FIGURE 9. TIME DISTRIBUTIONS OF B_θ (UPPER TRACE) AND E_z (LOWER TRACE) FOR THE MARK I GUN, AT THREE AXIAL POSITIONS AND THE SAME RADIUS. $B_\theta = 1.36 \text{ KGAUSS/LARGE DIVISION}$, $E_z = 0.52 \text{ STATVOLTS/LARGE DIVISION}$. $t = 0.2\mu \text{ secs/cm}$.

i.e., nearly 100% efficiency would be implied. A simple observation of the amplitude of the ringing current in the capacitor leads one to conclude, however, that 10% efficiency could not have been exceeded.

An important conclusion to be drawn from this result is that the identification of a moving current distribution, a moving luminous front, or even a moving charge distribution (which would have also been seen as such using doppler microwave techniques) with an actual motion of plasma is very hazardous, indeed.

A further result of interest is that shown in the B_θ and E_z plot for $t = 0.9 \mu\text{sec}$. Here, B_θ at the rear of the gun has begun to drop since the current in the external circuit is oscillating back toward zero. The result is positive gradient of B_θ in the region of $z = 8$ to 12 cm, and this should produce a backward acceleration of the plasma. We observe, in agreement with this conclusion, that E_z has changed sign, as it must if our conjecture as to the origin of E_z is correct at all. The fact that the E_z reversal occurs at the point of B_θ slope reversal also indicates that the amount of spurious noise or unbalance in the E_z measuring circuits is adequately small. There is a hint in the data of how large such "noise" might be, in that we note that the total number of ions in the distribution at $t = 0.6 \mu\text{sec}$, is actually shown to be larger than that at $0.5 \mu\text{sec}$, a rather unlikely result. Reference to the E_z curve for $t = 0.6$ shows that the E_z points used in computing n_1 were all just slightly greater than zero; a very slight downward displacement of the baseline would drastically reduce the value of n_1 , indicating that a zero error of this magnitude was probably involved. While this particular n_1 curve is somewhat shaky, (as also shown by the error bars) we may be fairly confident of the results obtained for the earlier times.

The physical situation which appears to exist, then, is that of a "wave" of current and ionization proceeding rapidly through the gas, and transferring some momentum to it, but not bringing the actual plasma velocity to anything like the desired value. In this regard, one important point related to the theoretical discussions of the introduction to this report must be made. It was stated that the rate of translational energy input to the

accelerating plasma is $\frac{1}{2} I^2 dL/dt$. The result was obtained using, by implication, a simple notion of a moving massive circuit boundary which moved along with the expanding current. In the present experiment the mass and the expanding circuit move separately; nevertheless, the rate of translational work on the plasma is still $\frac{1}{2} I^2 dL/dt$, where L is determined by the position of the current layer. This work term is simply another way of writing $\vec{F} \cdot \vec{v}$, and in this sense, we may just observe that in the experiment, \vec{F} is a "drag" force exerted on the ions which stream (relatively) past the current layer rather than a force representing the rate of change of momentum of mass resident in the current layer. It is not clear what determines the actual velocity of the current distribution, but for the given velocity, it is evident that the total plasma mass upon which the gun has chosen to break down is too large for attainment of $v = 10^7$ with the available energy.

At about the time the above experiments were completed, the components of the Mark II gun were available, and it was decided to defer the problem of the obvious propellant mass mismatch to the new apparatus.

2. Mark II

The Mark II gun was designed to have the lowest parasitic source inductance which could be attained with available components. It was decided to employ a capacitance of 1 μ fd, in order that compatibility with the eventual use of a high Q unit such as a vacuum capacitor would be maintained. The Axel Electronics Corporation of Jamaica, New York was able to supply capacitors of 0.1 μ fd, 20 kv rating whose natural ringing frequency was 3.0 mc. Our design then incorporated ten of these arranged in a circle, connected to the coaxial gun at the center by means of a parallel-plate transmission line. The rear circular plate was made heavy enough to serve as a mounting base and suspension for all the capacitors plus the gun. This gun, in its various stages of assembly, is shown in Figures 10 through 14, and a cross-sectional assembly drawing is given in Figure 15. Table I gives the barrel parameters for various modifications of the gun.

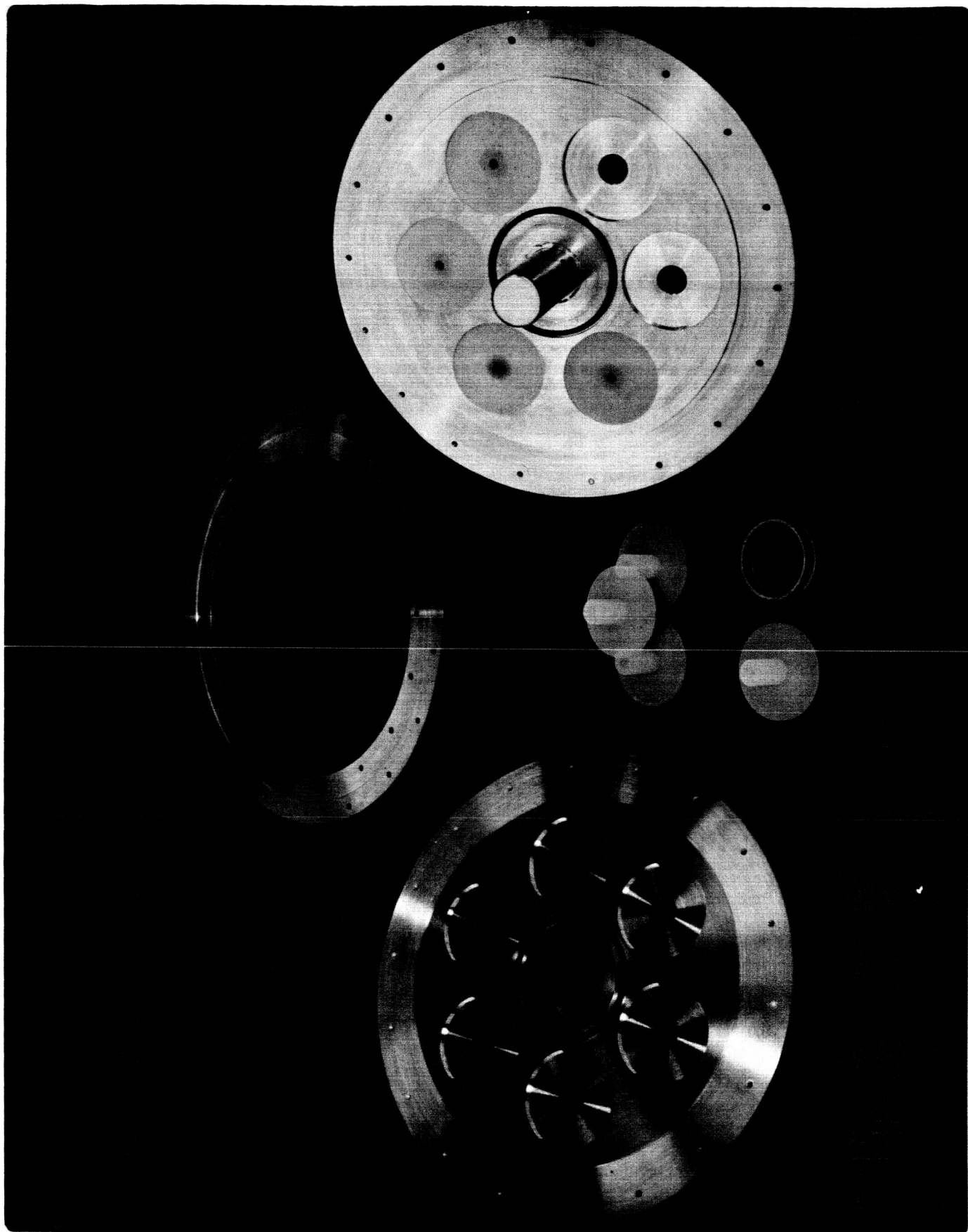


FIGURE 10. MARK II GUN

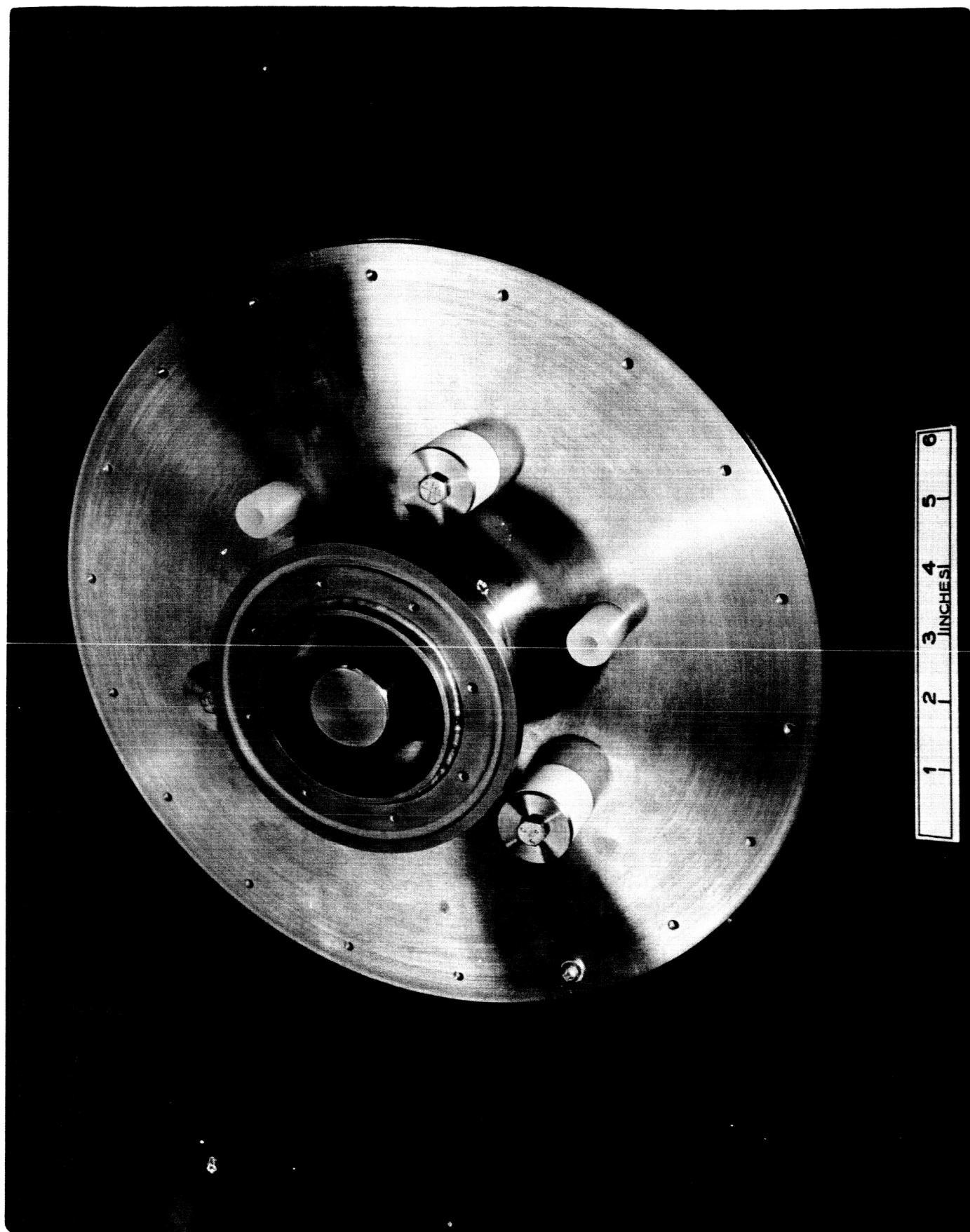


FIGURE 11. MARK II GUN

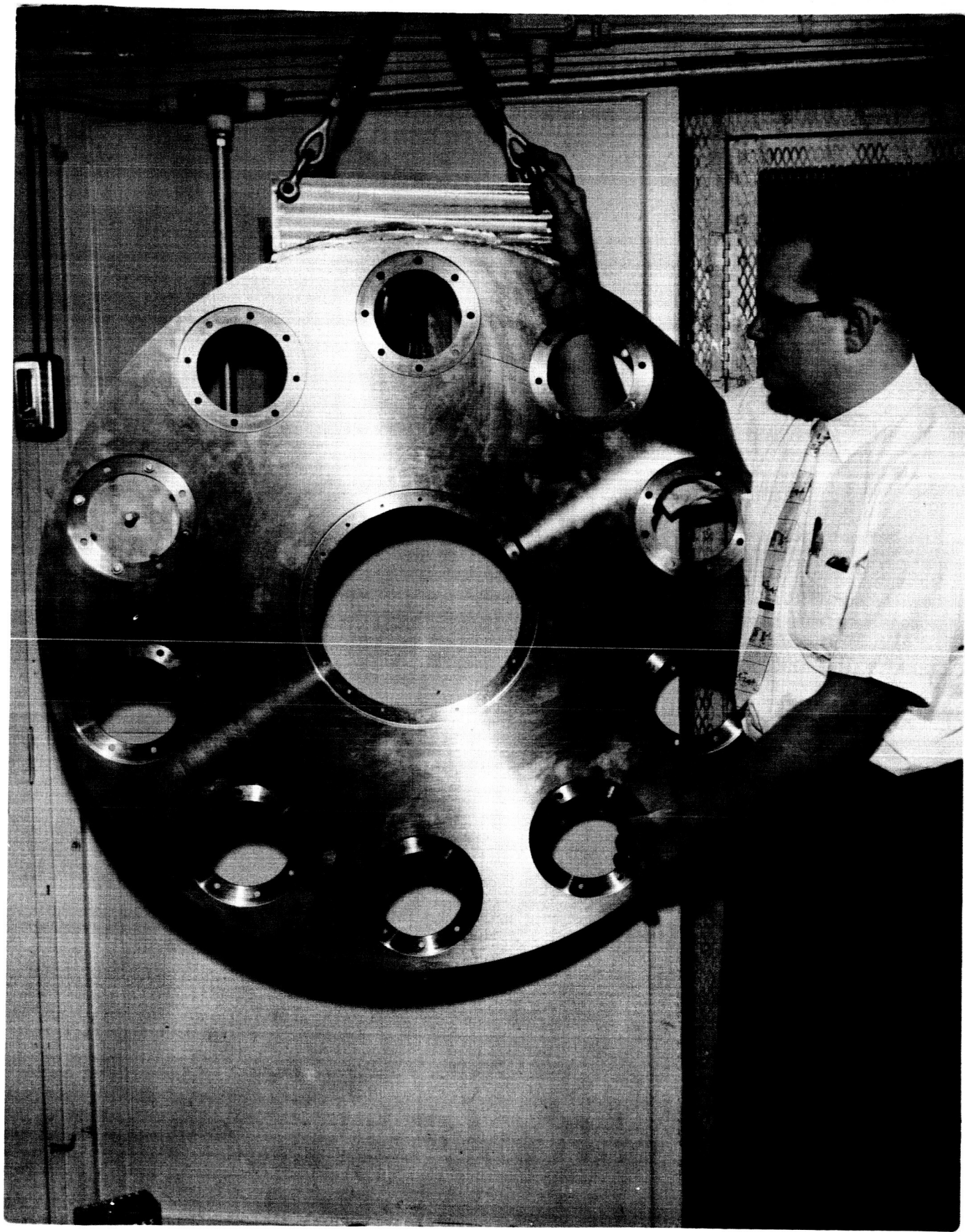


FIGURE 12. MARK II GUN

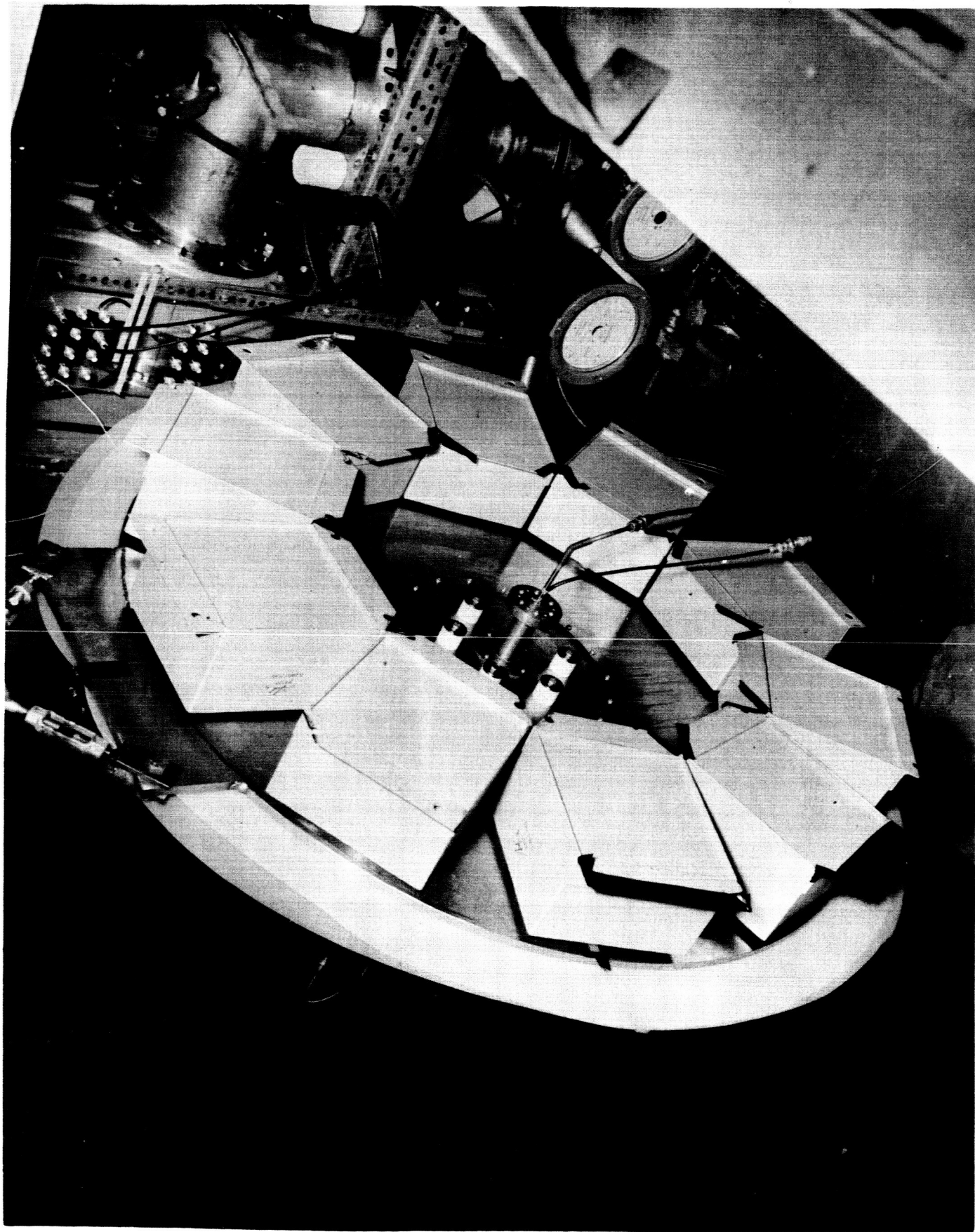


FIGURE 13. MARK II GUN

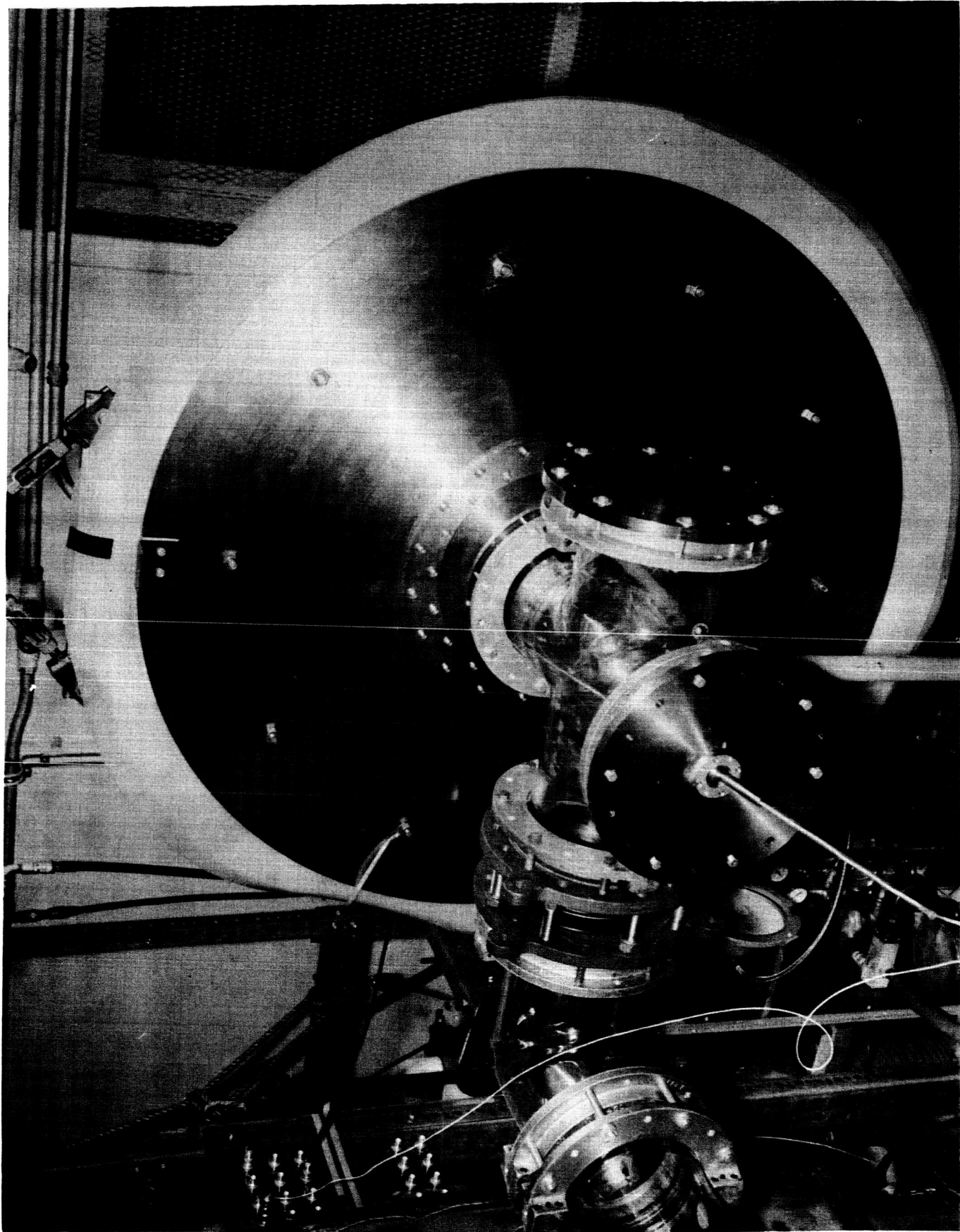


FIGURE 14. MARK II GUN

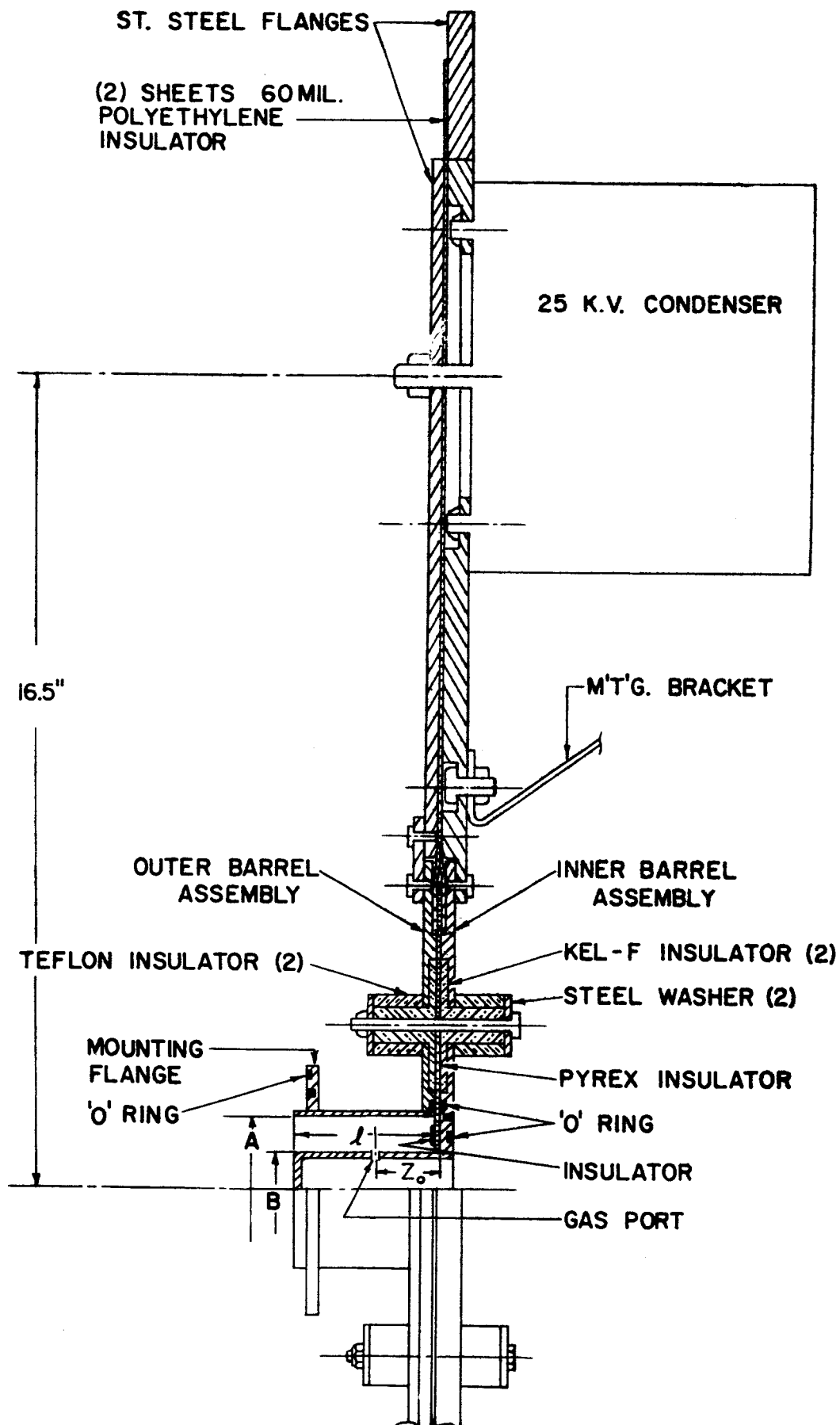


FIGURE 15. CROSS SECTION OF THE MARK II, III AND IV GUNS. THE DIMENSIONS A, B, l , z_0 FOR THE VARIOUS GUNS IS GIVEN IN TABLE I.

TABLE I
ELECTRICAL AND GEOMETRICAL GUN PARAMETERS

MODEL	CAPACITOR		DIMENSIONS (CMS)*				GAS PORTS	
	NO. OF UNITS	SIZE μ F	A	B	l	Z_o	NO. OF HOLES	HOLE DIAMETER (CMS)
I	1	1.6	8.25	3.81	33.4	10.5	10	0.635
II	10	0.1	7.80	3.73	8.25	2.54	80	0.102
III	10	0.5	7.80	3.73	8.25	2.54	25	0.318
IV	10	0.5	7.80	3.73	26.90	7.57	25	0.318

* The dimensions A, B, l , Z_o are illustrated in Figure 15.

The inductance of the ten capacitors in parallel as calculated from their ringing frequency, is 3×10^{-9} h. The transmission line, allowing for slightly more gap between the plates than the ideal $1/8$ " of the design is 2×10^{-9} h. Now the barrel adopted for this gun has inner and outer barrel radii of approximately 1.85 and 3.9 cm, respectively, which means an L' of 1.4×10^{-9} h/cm; in other words, the total external source inductance is equivalent to 3 cm of barrel length. Since the gas parts are located 2.5 cms out along the barrel, the $\Delta L/L_0$ efficiency criterion then requires that the acceleration of the plasma in this gun should take place over at least 6 cm of the length of the barrel. The total parasitic inductance is 8.5×10^{-9} h and the ringing frequency is then 1.7 Mc/s.

At this point, however, a difficulty arises, in that if one requires that $l/v = \sqrt{LC}$ where $L = \ell L'$, as given previously, the barrel length ℓ corresponding to $C = 1 \mu\text{fd}$ and $v = 10^7$ cm/sec is only about 1.4 mm! If instead, we ask for acceleration over a full electrical period, such that $l/v = 2\pi\sqrt{LC}$, ℓ turns out to be about 5.5 cms. In any event, it was clear that we would probably not satisfy $\Delta L/L_0 > 1$ by a large margin.

In the actual design of the gun, it was felt that while the external inductance had still not been reduced as far as would have been ideal the attainable $\Delta L/L_0$ would probably be great enough to give evidence of more efficient operation, e.g., some asymmetrical distortion of the current wave-form away from sinusoidal. (Asymmetry of the current wave-form is not a sufficient indicator of efficiency, however, since instabilities can also result in large ΔL .) Furthermore, all the advantages of low thermal losses due to short transmit time in the barrel, together with the favorable scaling with respect to the interchange (Rayleigh-Taylor) instabilities, should be obtained with a short barrel length. For mechanical convenience, as well as to take advantage of possible full-cycle operation, the barrel was made about 8 cm long.

Initial attempts to operate this gun were unsuccessful because of leakage conductance which appeared across the Al_2O_3 sheet insulator after a few shots. This conductance became high enough to prevent charging of the capacitor. After it was concluded that simple cleaning would not suffice,

and also that the insulator conductance was actually a metallic deposit from the electrodes, an extra insulating array, designed to shield the original sheet against sputtered metallic deposits, was installed. This arrangement, shown in Figure 16, was successful, and allowed steady operation except for occasional fractures of these glass shadow rings by pre-firing of the gun.

Initial probe runs and current traces showed no sign either of significant total inductance change, or even of plasma acceleration in the barrel. These data, as those in the Mark I, were obtained using argon, and on the assumption that the difficulty may again have been that too heavy a gas load was present at breakdown, a set of data were taken with Hydrogen as the propellant, the idea being that since the ionization potentials were not too different, one might expect a discharge on roughly the same number of atoms, and consequently, a much lighter mass loading. The result was a discharge which propagated rapidly down the barrel, and produced a strikingly asymmetric current wave, indicative of a large inductance change. The E_z field observed during the discharge implied that here the Hydrogen ions were being accelerated to something like the 10^7 cm/sec current sheet velocity.

While this result was encouraging in that it appeared to bear out the diagnosis of the trouble in accelerating argon, it was not itself a cure, since for reasons of high ionization and dissociation loss, as mentioned before, Hydrogen cannot be considered as a propellant for spaceflight applications, at least not for values of I_{sp} of less than 10,000 sec. At this point, however, a search for propellants lighter than argon was undertaken. Since we desired to avoid for the moment the technical difficulties of alkali metals, lithium was not considered. Helium represented a possibility in spite of difficult ultimate storage problems, but in trials in the gun, proved extremely erratic in its discharge characteristics, a result which is probably due in some measure to the very high ionization potential. Finally, it was decided to employ Nitrogen, since it is extremely easy to obtain, handle, and store, and is the lightest element heavier than Hydrogen having these properties.

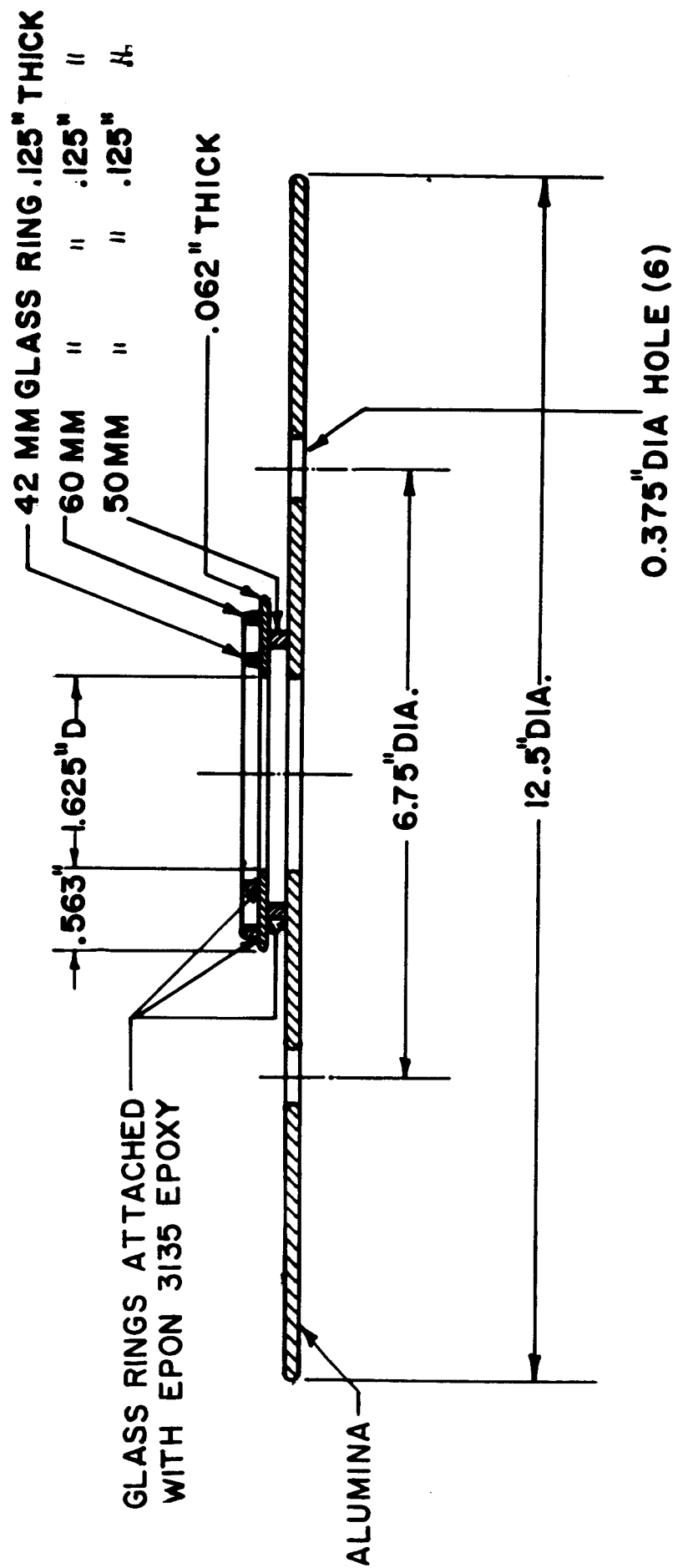


FIGURE 16. THE INSULATOR ASSEMBLY. THE GLASS RINGS SHIELD THE CENTRE AREA OF THE ALUMINA EXPOSED TO THE PLASMA, AND PREVENTS A CONDUCTING LAYER FORMING ACROSS THE INSULATOR.

When N_2 was put into the gun, it was clear that acceleration of the plasma was being obtained. However, the E_z time integrals were again not sufficiently large, and plasma velocities were apparently no greater than 3×10^6 cm/sec.

Figure 17 is representative of these results. There is no simple current layer detachment and forward propagation; rather the "toe" of the B_θ distribution moves outward at a slow rate, and most of the information on plasma acceleration is contained in the E_z curves. Of special interest is the plot for $t = 0.1 \mu\text{sec}$, where E_z is considerably larger than it is at later times; this is due to the incomplete ionization of the gas at this instant. The low ion density, together with a fairly large $\vec{j} \times \vec{B}$, result in large acceleration per ion and consequently large E . It will be noted that there is a sharp dip in E_z at about $z = 3.5$ just beyond the position of the gas ports, indicative of n_1 being peaked here. This is clear evidence that the initial breakdown occurred near the gas ports, and later as seen from the plots for later times, transferred to the insulator. Computed ion densities for this run are between 2 and 4×10^{15} per c.c., and these are fairly uniform, i.e., there does not appear to be a peaking, as in the Mark I data.

An unavoidable conclusion from these results is that even for nitrogen, a serious mismatch exists between the electrical system and the plasma mass. Clearly, ΔL is still a small number for the data shown above. On the basis of the trial run with Hydrogen, it might be concluded that the mass of N_2 is about an order of magnitude too high, in which case one might attempt remedies of two separate kinds: first, to attempt to induce early breakdown by external means such as magnetic fields and irradiation of the gas, or alternatively, to adjust other system parameters to improve the matching.

We recall that an approximate matching of the propellant to the gun was previously defined by

$$\kappa = \frac{c^2 V_0^2 L'}{2mz_0} \sim 1.$$

If m is indeed an order of magnitude high, we may consider an adjustment of

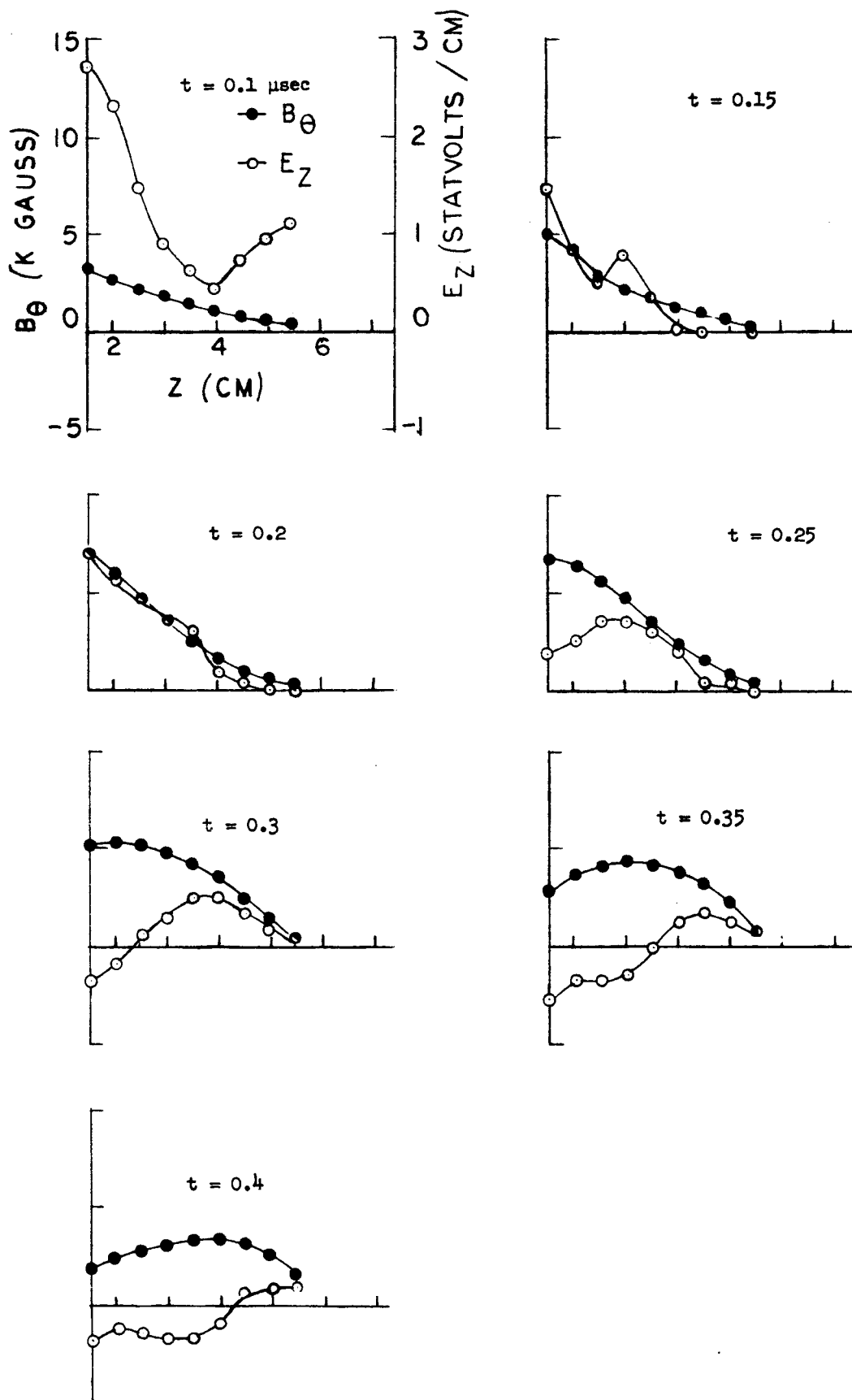


FIG. 17. DISTRIBUTIONS OF B_θ and E_z FOR THE MARK II GUN AT 14 KV. THE GAS PORTS ARE AT $z = 2.5$ CMS. TIME $t = 0$ CORRESPONDS TO THE START OF THE CURRENT RISE.

some other parameter in κ , since as has been seen, m is hard to control. Both V_0 and L' are hard to raise much above already used values, since L varies only as $\log b/a$ and V_0 much larger than the 15 to 20 kv range places severe demands upon the internal gun insulator. The initial discharge coordinate z_0 would have to be lowered, and this is clearly impossible here. The capacitance C remains as the single variable which can influence the match sensitively and in the right direction.

An upward adjustment of C represents a retreat from our previous stand at a one microfarad maximum; however, a decision was made to take this step, since it appeared more important at this time to prove the gun concept in principle, than to be too severely constrained by engineering considerations. Accordingly, an order was placed for a set of 0.5 μfd , 25 kv units (Axel) which were, except for capacitance and depth of the cans, identical to the 0.1 μfd capacitors. The new combination of parameters was dubbed Mark III.

3. Mark III

A simple qualitative argument serves to demonstrate how strong an effect this upward adjustment of C might be expected to have, assuming no inductance change in the capacitor. We list several quantities of importance, together with their factors of increase:

B	\times	$\sqrt{5}$
Force ($\sim B^2$)	\times	5
Period (τ_0)	\times	$\sqrt{5}$
Momentum ($=F \cdot \tau_0$)	\times	5 $\sqrt{5}$
Energy [$\sim (F\tau_0)^2$] (since m is constant)	\times	125
Stored energy (W_0)	\times	5
Efficiency $\frac{(F\tau)^2}{W_0}$	\times	25

Experimental data taken with the Mark III configuration appear to bear these qualitative predictions out completely. In Figure 18 are pre-

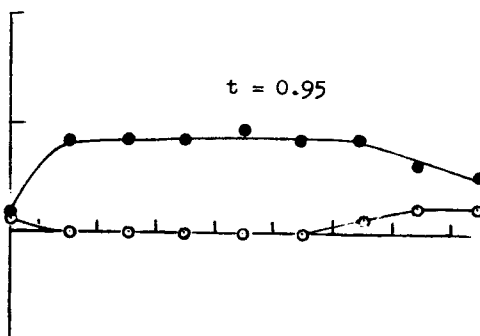
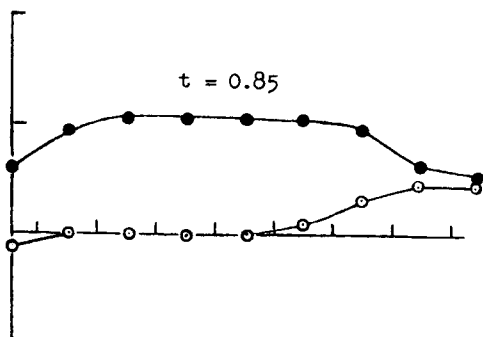
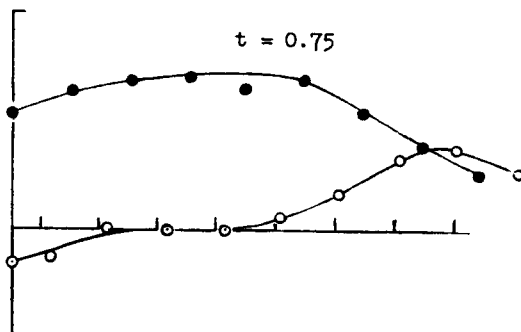
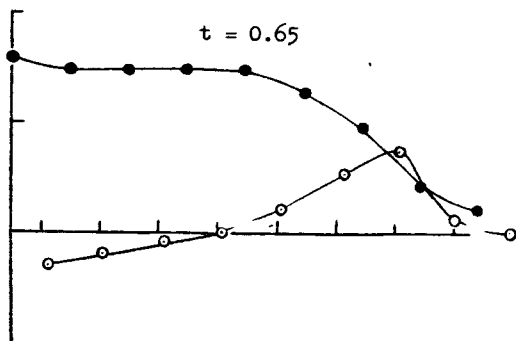
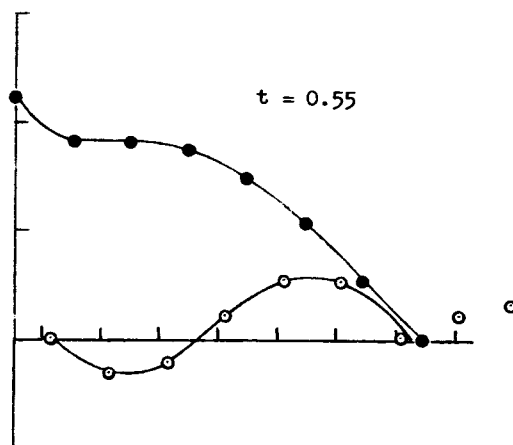
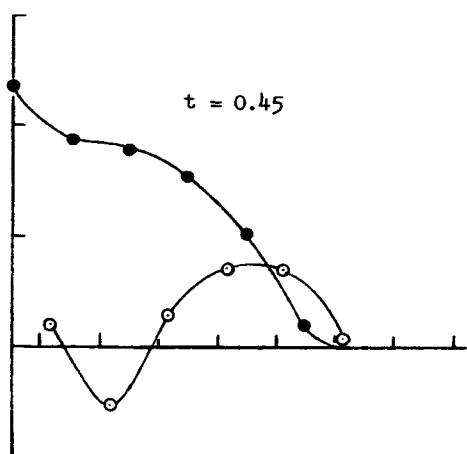
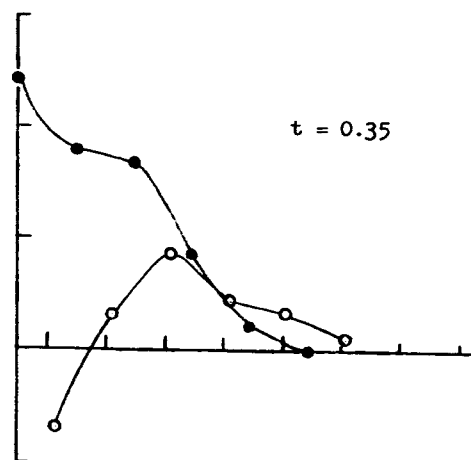
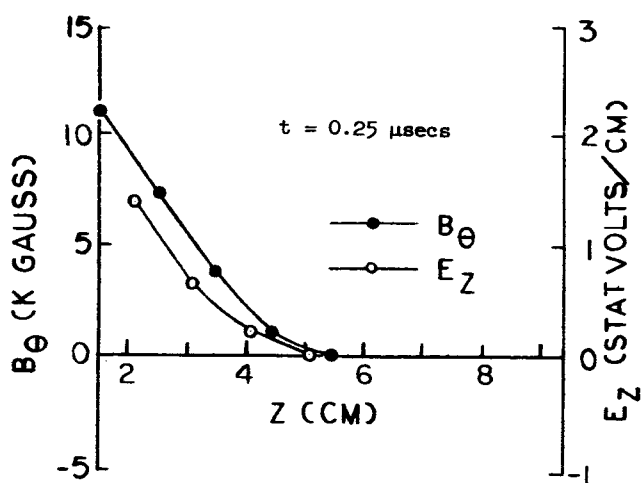


FIG. 18. DISTRIBUTIONS OF B_θ AND E_z FOR THE MARK III GUN AT 14 KV. THE GAS PORTS ARE AT $z = 2.5$ CM. TIME $t = 0$ CORRESPONDS TO THE START OF THE CURRENT RISE.

sented data which may be compared directly with those of Figure 17 for Mk II. The plots are on the same distance and amplitude scales, but are done at different time intervals.

One sees that in Mark III, the fields at 0.25 μ sec look roughly like those in Mark II, except that in the latter, B_θ near the rear has begun to ring back toward zero, and the resulting reduction in slope has dropped E_z somewhat. However, the continuing current rise in the new gun rapidly produces a detached current layer which moves toward the muzzle at 10^7 cm/sec.

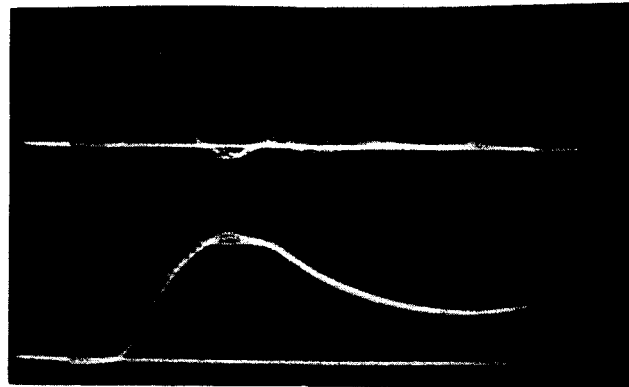
The total energy imparted to the plasma is about $\int \Delta(B^2/2\mu_0) dz$, integrated over the area of the current sheet, where $\Delta(\frac{B^2}{2\mu_0})$ is the magnetic pressure drop across the current sheet, and dz is an increment of current sheet travel. This is exactly equivalent to $\frac{1}{2} I^2 \partial L / \partial t$ integrated over the transit time of the sheet down the barrel, and by the same arguments used previously, is quite independent of whether the ions follow at the current layer speed or not. Since the B_θ distribution in Mark II moves so little, this integral is difficult to estimate; however, it appears that the energy transfer in Mark III, as estimated in this way is at least two orders of magnitude greater.

It seems, from the E_z data for Mark III, that in this instance, the ions are actually moving at a velocity comparable to that of the current layer. A field of about 1 esu/cm is moving along with the current, and this is approximately the field which, if applied for the transit time, would accelerate a Nitrogen ion to 10^7 cm/sec.

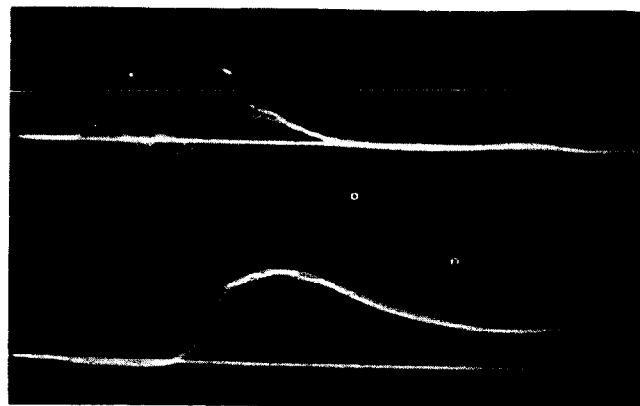
In Figure 19 are four sets of B_θ and E_z traces for different positions along the barrel. The delayed rise of B_θ with advancing z demonstrates the current sheet propagation, and a pulse of E_z is seen to accompany the current. As is plain from the plots of Figure 18, however, the acceleration is far from complete when the current reaches the end of the gun. We have followed its progress beyond the muzzle ($z = 8.0$), and find that the acceleration is continuing in a normal manner in the plume which extends out to twice this distance. Figure 20 shows B and E for two external positions. Note that the reproducibility of the traces is still excellent in the plume, an indication of good stability.



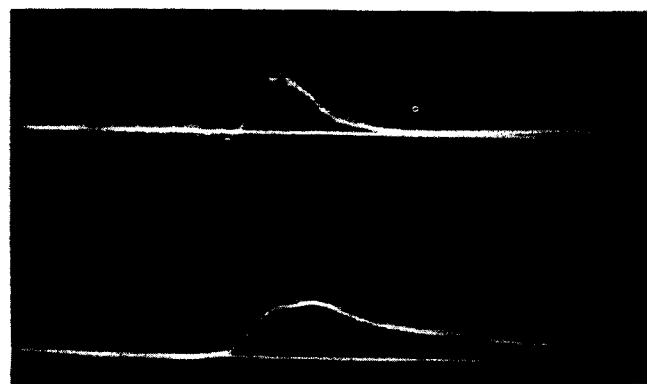
$z = 1.5 \text{ cms}$



$z = 3.5 \text{ cms}$



$z = 5.5 \text{ cms}$

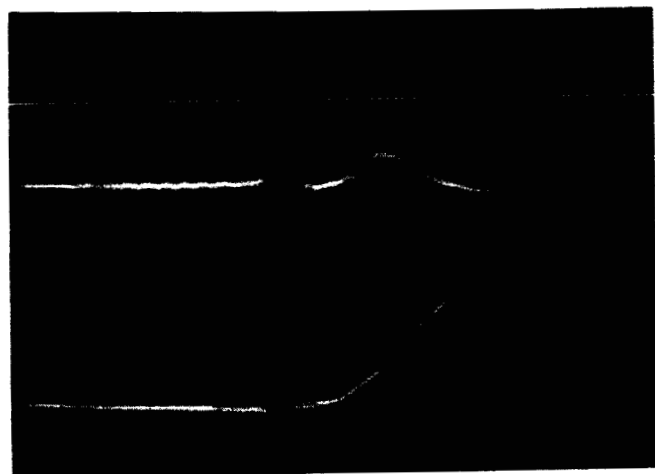


$z = 7.5 \text{ cms}$

FIGURE 19. TIME DISTRIBUTION OF B_{θ} (LOWER TRACE) AND E_z (UPPER TRACE). $B_{\theta} = 4.8 \text{ KGAUSS/LARGE DIVISION}$, $E_z = 0.95 \text{ STATVOLTS/LARGE DIVISION}$. $t = 0.2 \mu\text{secs/cm}$. THE MUZZLE OF THE GUN IS AT $z = 8.0 \text{ cms}$.



$z = 9.5 \text{ cm}$



$z = 11.5 \text{ cm}$

FIGURE 20. TIME DISTRIBUTION OF B_θ (LOWER TRACE) AND E_z (UPPER TRACE) BEYOND THE MUZZLE OF THE GUN. $B_\theta = 0.96$ KGAUSS/LARGE DIVISION, $E_z = 0.95$ STATVOLTS/LARGE DIVISION. $t = 0.2\mu \text{ secs/cm.}$

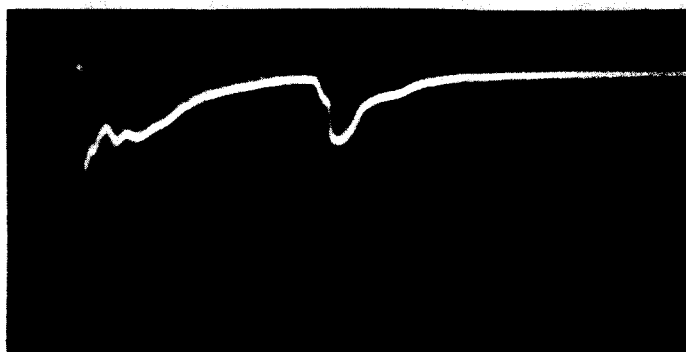
We have obtained, inadvertently, an indication of actual plasma velocity which is independent of probe data. It was noticed during the preliminary setting-up of a monochromator for spectral studies, that when the instrument was sighted toward the gun along its axis, two distinct flashes of light occurred, one at the time of the discharge, and the other several microseconds later, when the energy in the gun had long since decayed to zero. By simply moving the position of the vacuum window away from the gun, it was verified that the second flash resulted from the plasma striking this window. Since the transit time was long compared with either the gun discharge time or the rise time of the second flash, it was possible to estimate the plasma velocity by dividing the drift distance by the delay time. In Figure 21, the monochromator output is shown for three different gun voltages. The plasma velocity and gun voltage appear to be linearly related, as simple scaling would predict, although zero velocity corresponds to somewhat more than zero voltage. These results are plotted in Figure 22.

The velocity of the current sheet, as determined from probes, was also measured for several voltages. Surprisingly, it proved to be independent of voltage as shown in Figure 23. However, the plasma velocity calculated from E_z agreed with that obtained optically. The inference to be drawn seems to be that as the voltage on the gun is increased, the current sheet acts increasingly like a tight "snowplow", and that at the higher voltages, the plasma is actually achieving the desired speed.

While the transfer of energy from the field to the propellant appears to proceed fairly efficiently in this device, there is one aspect of its behavior which prevents high overall efficiency; this is the tendency to "crowbar", or set up secondary discharges at the insulator of the gun. Such short-circuiting prevents the flow of energy from the bank to the barrel, and vice versa, with the result that the portion of the energy which is thus sealed off in the bank and external circuitry must simply dissipate in circuit resistance. This might not be intolerable if the crowbarring occurred at zero bank voltage, (near current maximum) and the fraction of the total magnetic energy left outside were small. However, this is not the case in our device. As seen in the B_θ plots of Figure 18, crowbarring is occurring



18K Volts



14K Volts



12K Volts

FIG. 21. TIME DISTRIBUTION OF THE INTENSITY OF THE 4094
ANGSTROM LINE. $t = 2.0 \mu\text{SEC}/\text{CM}$. THE SECOND PEAK
OCCURS WHEN THE PLASMA STRIKES A GLASS PLATE
50 CMS FROM THE MUZZLE OF THE GUN.

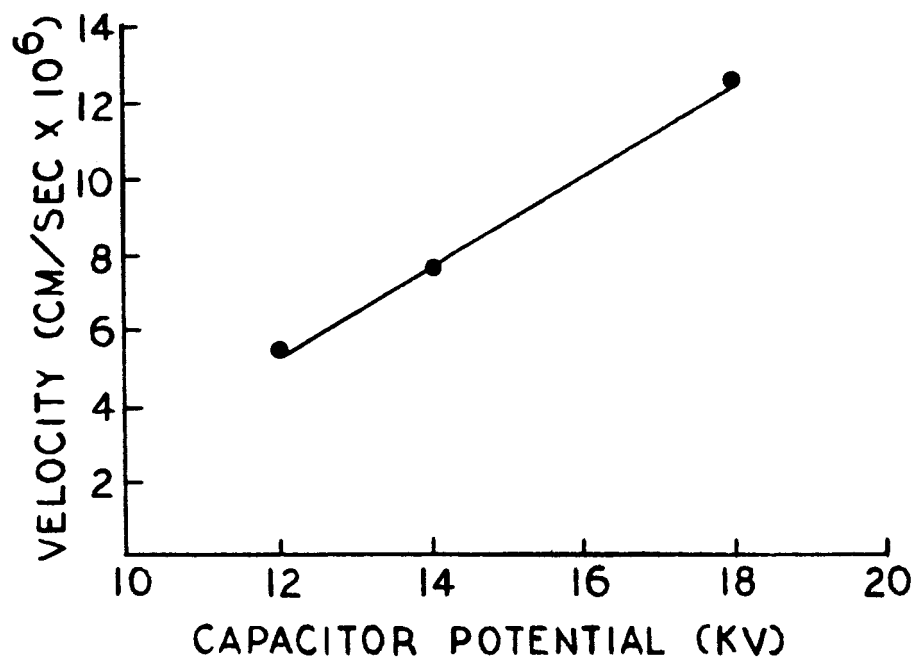


FIG. 22. THE PLASMA VELOCITY DETERMINED FROM THE MONOCHROMATOR DATA SHOWN IN FIGURE 21.

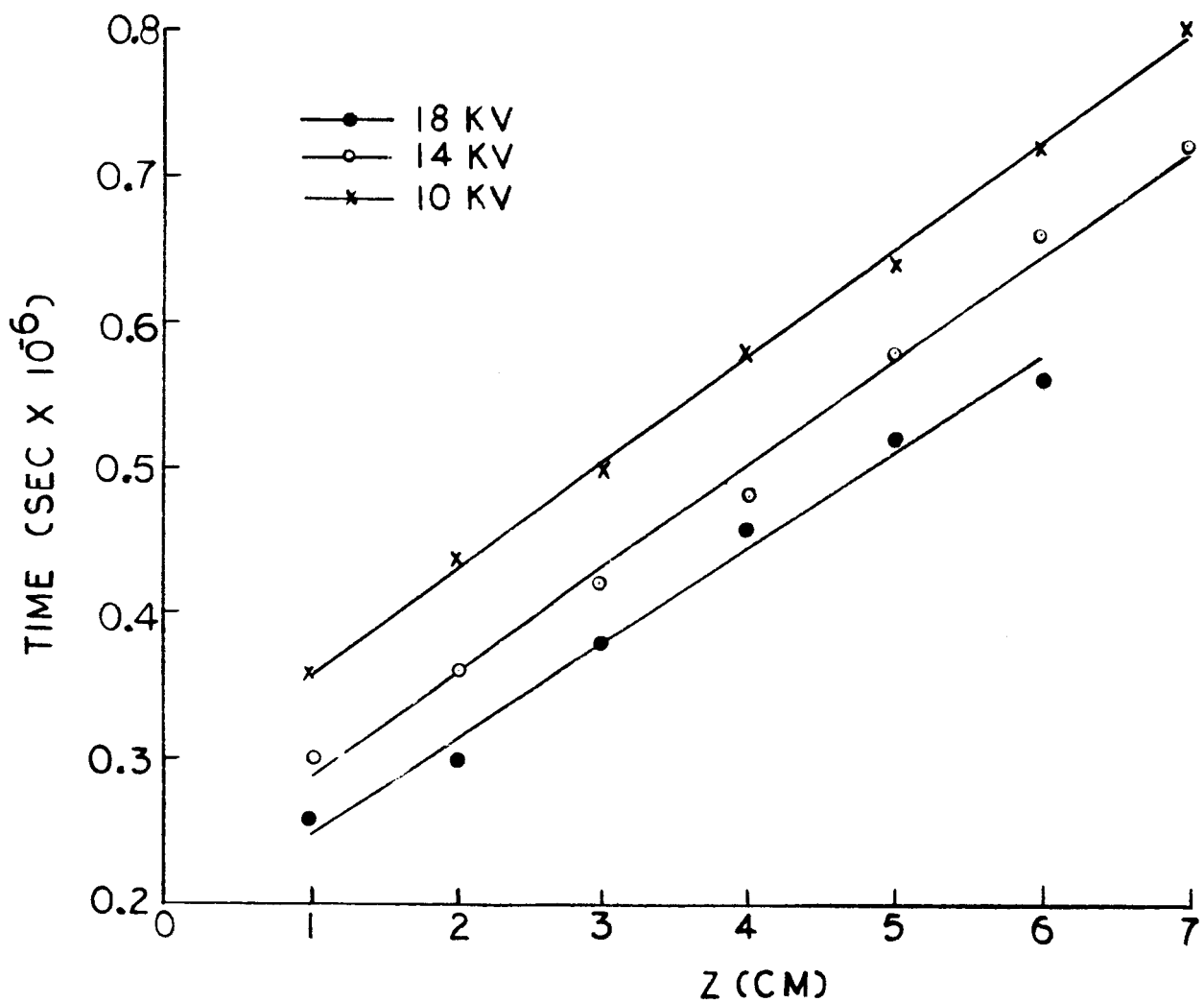


FIG. 23. THE POSITION OF THE CURRENT SHEET AS DETERMINED BY THE RISE IN E_z . THE SLOPES OF THESE CURVES REPRESENT THE SHEET VELOCITY.

at 0.35 μ sec, when the current is still rising, and thus efficiency is drastically lowered, since in addition to maximum current not being achieved in the plasma, the external inductance exceeds the internal inductance at this time. This crowbarring can be observed directly by comparing the shape of the $B(t)$ distribution at a fixed position close to the insulator, with the external current. In Figure 24, $B(t)$ follows $I(t)$ for 0.2 μ secs then breaks, indicating that a current sheet has formed between the probe and the insulator.

4. Ballistic Pendulum Measurements

Although we had not relied to any extent on external momentum measuring procedures up to this point in the program, it seemed worthwhile to expend the small effort needed to install a calorimeter-type ballistic pendulum in front of the gun.

There are several reasons why we have felt that pendulum data in this application must be suspect. Principal among them is the fact, as seen in the previous data, that the plasma, upon emerging from the gun, does not usually disconnect itself electrically from the gun, but rather draws after it a long plume of current. When the plasma is stopped by a pendulum there can then be a direct transfer of momentum from the associated magnetic field rather than from the kinetic momentum of the gas itself, and an erroneously high indication can result. The calorimeter technique for the measurement of plasma energy is only valid if the plasma makes a completely inelastic collision with the barrier, and if all of the incident energy is transferred to pendulum heat; it is useful, however, in that it places a lower limit on the plasma energy.

With these problems in mind, we hung a simple copper sheet pendulum at a distance of 25 cm from the muzzle of the gun. The general arrangement is shown in Figure 25. Both temperature rise and deflection were measured, although generally not for the same shot. For these runs, the conditions for the run of Figure 18 were used.

The proper mass for the first pendulum tried was estimated by using the measured plasma velocity times a plasma mass obtained by the E and B determination of n_1 and the approximate volume (100 cm^3) occupied by the gas

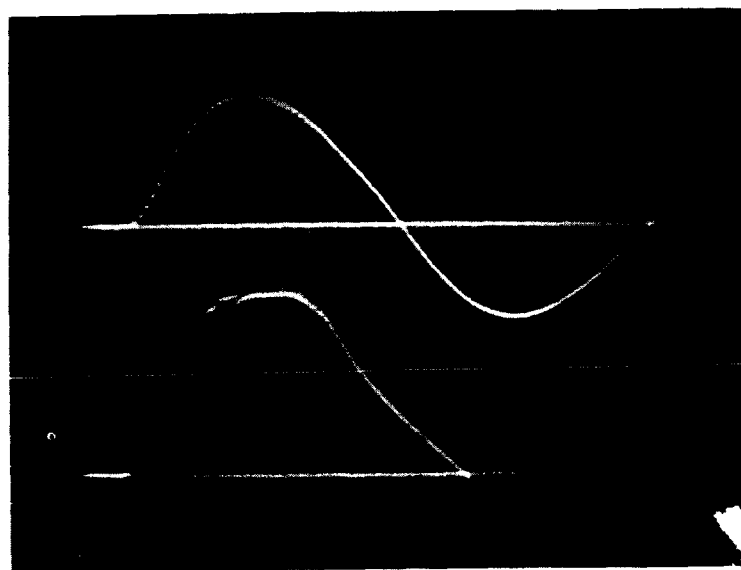


FIGURE 24. TIME DISTRIBUTION OF THE TOTAL CURRENT I (UPPER TRACE) AND B_{θ} (LOWER TRACE) FOR THE MARK III GUN AT 14 KV. AND 350 MM NITROGEN. THE B_{θ} PROBE IS AT $z = 1$ cm, TIME SCALE = $0.2 \mu\text{secs/cm}$.

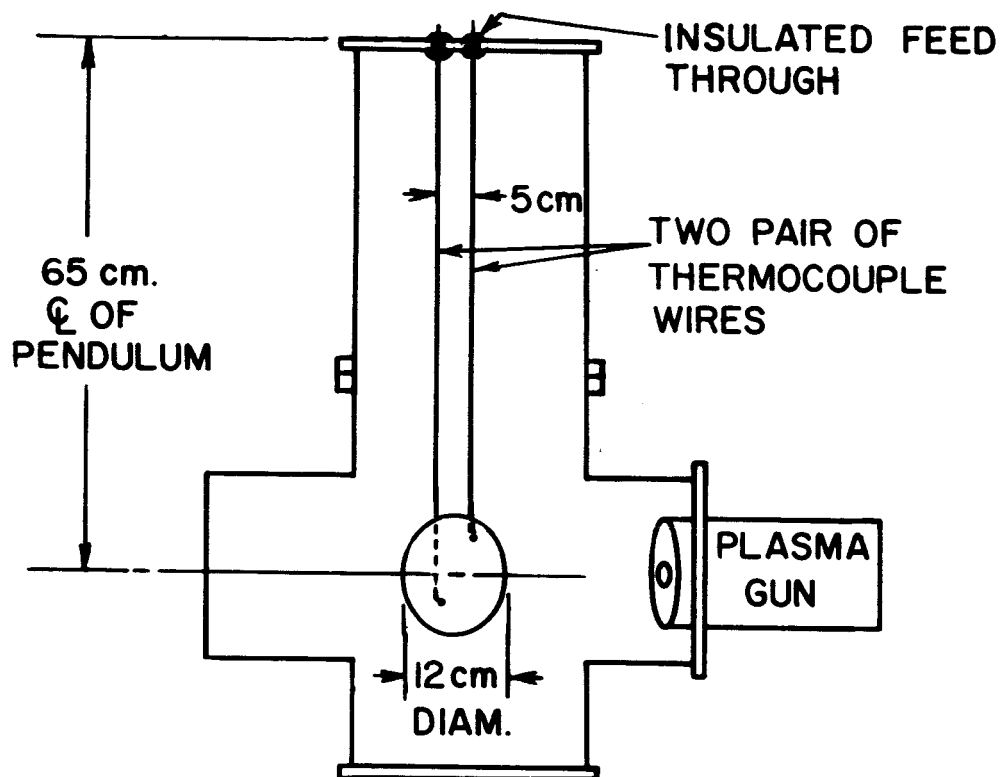


FIG. 25. THE PENDULUM ARRANGEMENT

at the firing time. This momentum, together with a convenient deflection amplitude, determined the pendulum mass. When the gun was fired onto this disk, a very large deflection resulted, and not until the mass was increased a factor of ten did the deflection attain the desired level.

The parameter values applicable to experiments with this modified pendulum were:

Mass	68 g (Cu)
Suspension length	65 cm
Disk diameter	12 cm
Distance from gun	25 cm
Deflection (average)	1.6 cm
Spread of deflections	± 0.1 cm
Temperature rise/shot	2.5°C
Spread in ΔT	$\pm 0.5^\circ\text{C}$
Calculated momentum transfer	425 g-cm/sec
Calculated heat transfer	75 joules

The estimates of what plasma energy and momentum should be cannot be made to much better than a factor of two. These estimates, made prior to the pendulum shots were: energy, ~ 70 joules; momentum, ~ 80 g-cm/sec. The measured energy transfer is very close to the estimate, but the momentum transfer is about a factor of five too high.

The direct B-field pressure hypothesis seemed to be a reasonable way of explaining the discrepancy, and so, a pair of holes were drilled in the pendulum plate through which magnetic probes were inserted. It was found that as expected, B-field "piled up" against the pendulum, together with the plasma in which it was imbedded; nevertheless, the magnitude was only enough to account for an error of perhaps a factor of two.

We then investigated the possibility that the rapid rate of energy delivery to the pendulum face was heating a thin surface layer to beyond the boiling point and ejecting a cloud of vaporized copper whose momentum

was actually being measured. In this case, the evaporated material would be much more massive, but moving far slower than the incident plasma. In order to isolate this effect, a thin layer of Mylar was placed over the pendulum face. This material by virtue of its lower heat conductivity and lower boiling point, might be expected to produce an even stronger "ablation effect". Such a result was then indeed observed in that the deflection, even for the increased mass, was nearly doubled with the Mylar face. Further substitutions of face materials verified in this interpretation of the deflection anomaly. Representative values for different materials normalized to a mass of 68 gms are the following:

<u>Material</u>	<u>Deflection (cm)</u>
Cu	1.6
Ta	1.8
Mylar	2.4
Mica	2.6
Cu, coated with black wax	2.9

It was also noticed that for the same material, the first shot fired after some appreciable interval gave a significantly larger deflection, typically 20% larger, than those from subsequent shots fired in close (~ 1 min) sequence afterward. This was interpreted as being due to the ejection of gas occluded on the surface.

The ablation hypothesis was further confirmed by observed mass loss from the pendulum, and a nearly opaque coating of the glassware near the pendulum position. In one instant, 15×10^{-3} gm mass loss was measured after five shots from the gun.

While this experiment was done in very rough and preliminary fashion, it constitutes adequate proof of the unreliability of the ballistic pendulum technique. It seems worthwhile to bear on this point rather heavily, since claims of high MHD engine efficiency have been repeatedly made on the basis of such measurements.

With regard to the thermal measurement, one further point may be made.

If in Figure 18, we integrate $B^2/2\mu_0$ over the length of the barrel and the cross-section of the tube, we obtain an energy transfer $\left(\frac{1}{2} I^2 \frac{\partial L}{\partial t}\right)$ of a little over 50 joules. This figure agrees when adjusted for the voltage ratio with the 75 joule figure obtained from the pendulum heat rise, and constitutes, for purposes of this project, an extremely important piece of information. It is just that it appears possible to transfer the energy of the magnetic field into directed plasma kinetic energy with good efficiency. Losses to the electrodes and radiation losses are apparently not disastrous. As pointed out before, the overall efficiency of this gun has been held down by the crowbarring, but in our main area of concern, which is the efficiency of energy transfer from the field to the plasma motion, these results appear most encouraging.

5. Mark IV.

Since the crowbarring trouble at the rear insulator appeared to be an essential obstacle to the attainment of good energy transfer from the bank to the barrel, an attempt to alleviate this short-circuiting trouble was made through the expedient of increasing the spacing between the gas ports and insulator from 2.5 cm to 7.5 cms. The barrel was also extended to 20 cm beyond the gas ports. With this new spacing, it was hoped that the discharge would occur over the ports before enough gas had reached the rear to support an early insulator breakdown.

This change corresponds to an increase in the parasitic inductance of barrel from about 6 cm to 11 cm. In order, then, to bring κ to its previous value, it would be necessary to lower m by a factor of 6/11, or to raise V_0 by a factor of 1.35. Since the latter change is possible within the ratings of the system components, this change was not felt to be so great as to upset seriously whatever matching had existed in Mk III.

At just the time when the Mk IV components were being manufactured, the entire laboratory was moved to the General Dynamics/Astronautics site which is several miles distance from the original location. A delay in the program of three weeks resulted, and at the time of the writing of this report, full operation has just again been attained. Some preliminary data from Mk IV

are in hand, and these will be discussed below, although no detailed and final analyses of its operation have been made.

A front-view photograph of Mk IV is shown in Figure 26. Figures 27 through 29 show the new experimental layout in the General Dynamics/Astronautics plant.

The initial running of Mk IV demonstrates clearly that the crowbarring can be eliminated for the first half-cycle of current if (1) the voltage is held to less than about 20 kv, and (2) the gas influx rate from the ports is sufficiently fast so breakdown at the ports occurs before gas has reached the insulator. (The voltage restriction is no problem, since all previous running has been done at 14 to 18 kv.) If the gas flow is made too slow, however, the initial current flow is on the insulator. In this condition, we have observed what is probably a significant effect, i.e., that if the rear sheet insulator is of Pyrex, a serious attachment of the discharge occurs, but if an alumina (Al_2O_3) plate is used, even though it has Pyrex "shadow rings" cemented to it, the discharge moves promptly away from the insulator, even though it formed there.

A somewhat negative sort of behavior has been observed in this gun, however, in that the discharge shows some tendency toward instability after a few cms of travel. It is not clear yet whether this irregularity is serious in the sense that it has absorbed significant energy in its formation, i.e., that it has grown to large amplitude; we have so far only observed azimuthal asymmetry in B_θ at positions downstream from the gas ports. With the arrival of a 0.05 μ sec Kerr-Cell camera, we should be able to observe these instabilities directly.

6. Repetitive Firing Experiments

In section C, we have outlined an idealized operating sequence for multi-shot running of this gun. It assumes that immediately after a shot, the remaining gas deionizes in a time short compared with the refill time, so that the capacitor may re-charge.

A desirable re-charging scheme would, from the viewpoint of simplicity, require only passive networks and no programmed switching. The simplest

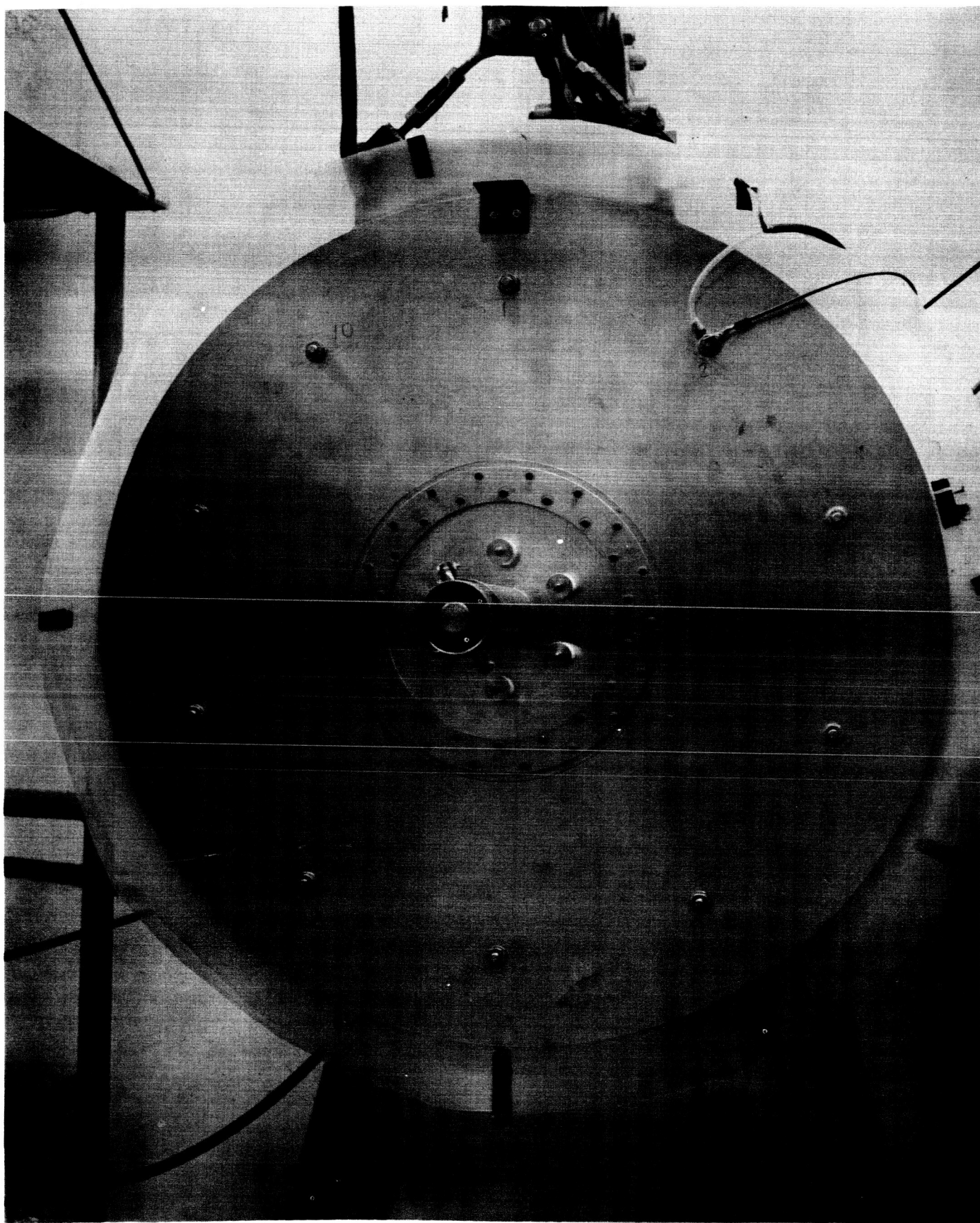


FIG. 26. THE MARK IV GUN

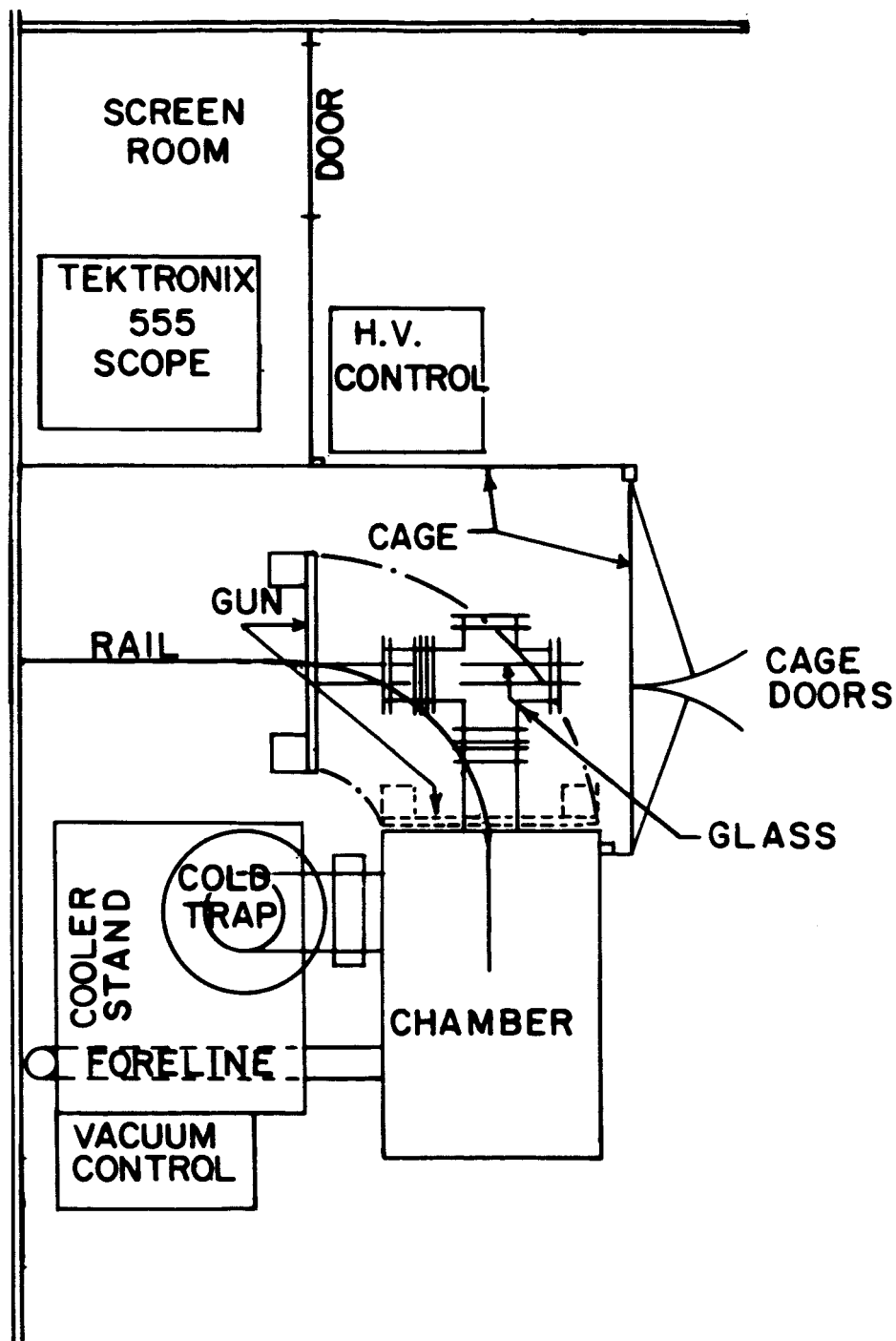


FIG. 27. THE EXPERIMENTAL ARRANGEMENT

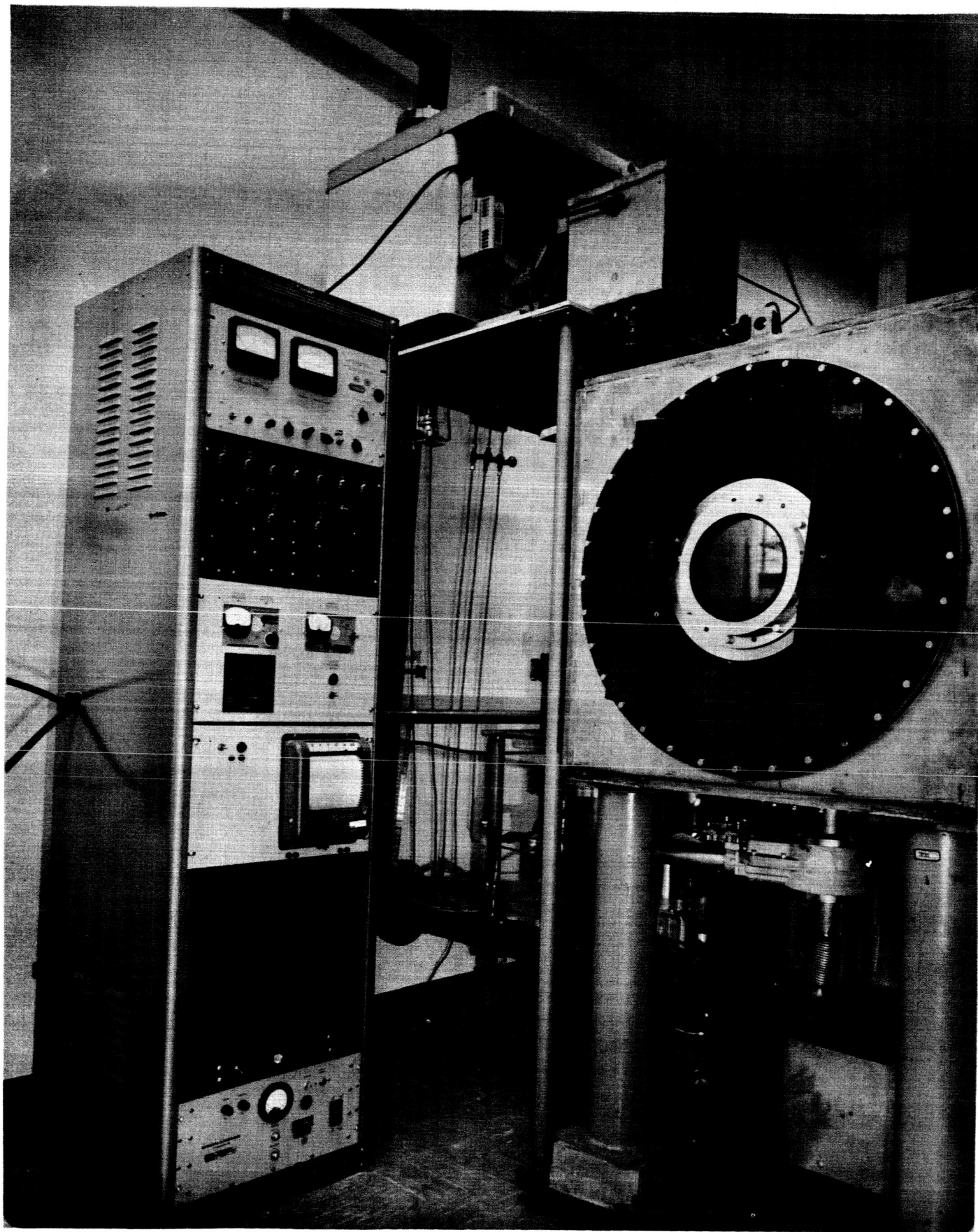


FIG. 28. THE VACUUM SYSTEM

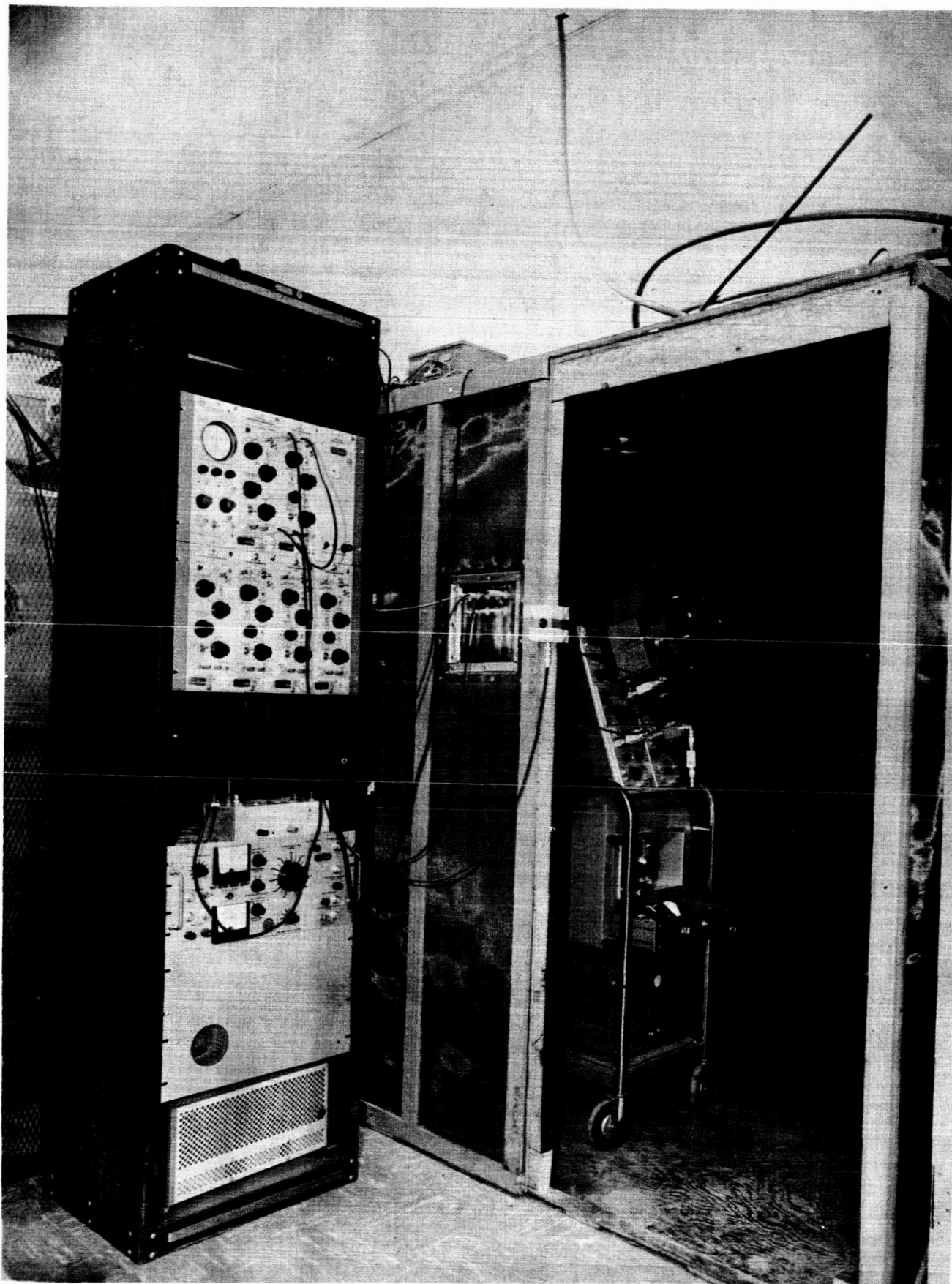


FIG. 29. THE CONTROL PANEL AND SCREENED ROOM

arrangement is a resistor between the power supply and the gun; this fails, not only because of its inefficiency - half of the input energy is dissipated in the resistor - but because immediately after a shot, a current V/R (V is the power supply voltage) is available to maintain a glow discharge in the barrel, and in order to maintain a high enough repetition rate, R cannot be too large. For example, if $C = 1 \mu\text{fd}$, and we operate at 10^3 shots/sec., RC must be about $100 \mu\text{sec}$, or $R = 100\Omega$. But then, 200 amperes of current can flow into an unquenched residual discharge, or afterglow, as well as into the capacitor.

The insertion of inductance into the charging line is a step in the right direction, since at early times after the shot, I grows just as Vt/L . There remains the possibility, however, that the afterglow may last long enough so that extremely large L would be required to keep I low until quenching.

We performed, using the Mk II gun, some experiments on the feasibility of such a re-charging scheme using Neon, Nitrogen, and Hydrogen as propellants. A $7.5 \mu\text{fd}$ capacitor was used as a "power supply", and for a first test a resistance was placed between it and the gun. If the gun had turned off after the shot, the result would have been about a 12% drop in the voltage on the re-charge capacitor. Instead, however, this capacitor was completely dumped after every shot indicating that the V/R current kept the discharge alive.

When inductances were inserted into the line also, it became apparent that inductance enough to turn off the discharge would make the full re-charge time much too long. We did not, in fact, have inductors of sufficiently high value to turn off the gun.

It was then realized that an excellent solution to this problem might be the use of a saturable reactor in the charging line. Such a device can have extremely high inductance up to the time the core saturates, and after that, the inductance drops precipitously. The result is that the re-charge current can be very small for some interval of time, after which it surges quickly to a high value. In a sense, this can be considered a delayed current switch.

The saturable reactor idea was tested by the use of a pulse transformer O-core of 1-1/2" x 1-1/2" cross-section, on which a multi-layer coil was wound. It displayed a very sharp break in current when used in charging the gun capacity. For example, at 300 μ secs. after the gun firing, the charging current was 70 ma; but 200 μ secs. later, it had risen to 3 amperes.

With this arrangement, we were able to produce "turning-off" of the gun although only erratically. It was necessary, for example, to use Hydrogen and also to run the gun at only 6 kv.

In order to further determine the factors influencing the quenching of the discharge, an ignitron switch was placed in the charging line (again, between the 7.5 μ fd re-charge capacitor, and the 1 μ fd gun) with a 75 ohm resistor in series with it. At variable times subsequent to gun firing, this ignitron was turned on, and the re-charge capacitor voltage observed for either complete dumping or the 12% drop which signified a gun quench. The result was that occasional voltage hold-off was observed, but only for very long delays. Furthermore, it was discovered that under the conditions of input gas flow and gun voltage where hold-off after the shot was observed, the main discharge had occurred out in the glass vacuum system beyond the end of the barrel. When the input gas flow rate was increased to a point where the internal current distribution in the barrel became normal, the gun would not hold off the re-charge voltage.

It appears that there is a fairly simple interpretation of these data, and it is that in this gun, there is still significant ionization of the residual gas when the cold entering gas has reached sufficient pressure for a new breakdown. That is, the necessary interval of time during which there is neither ionization nor a high neutral gas pressure does not exist. This time will depend on the recombination coefficients of the propellant. According to Brown's book⁶ N_2 has a much larger coefficient than Ar or Ne; however, the hold-off time, using N_2 , was still very long. It appears that unless a more efficient combination of gun parameters can succeed in ridding the barrel more completely of ionized gas at the time of the shot, it will be necessary to go to a pulsed gas valve.

Further tests on this problem were postponed until such efficient single-shot conditions might be found, since it was clear that the Mk II gun, as used here, left a considerable fraction of the plasma in the gun.

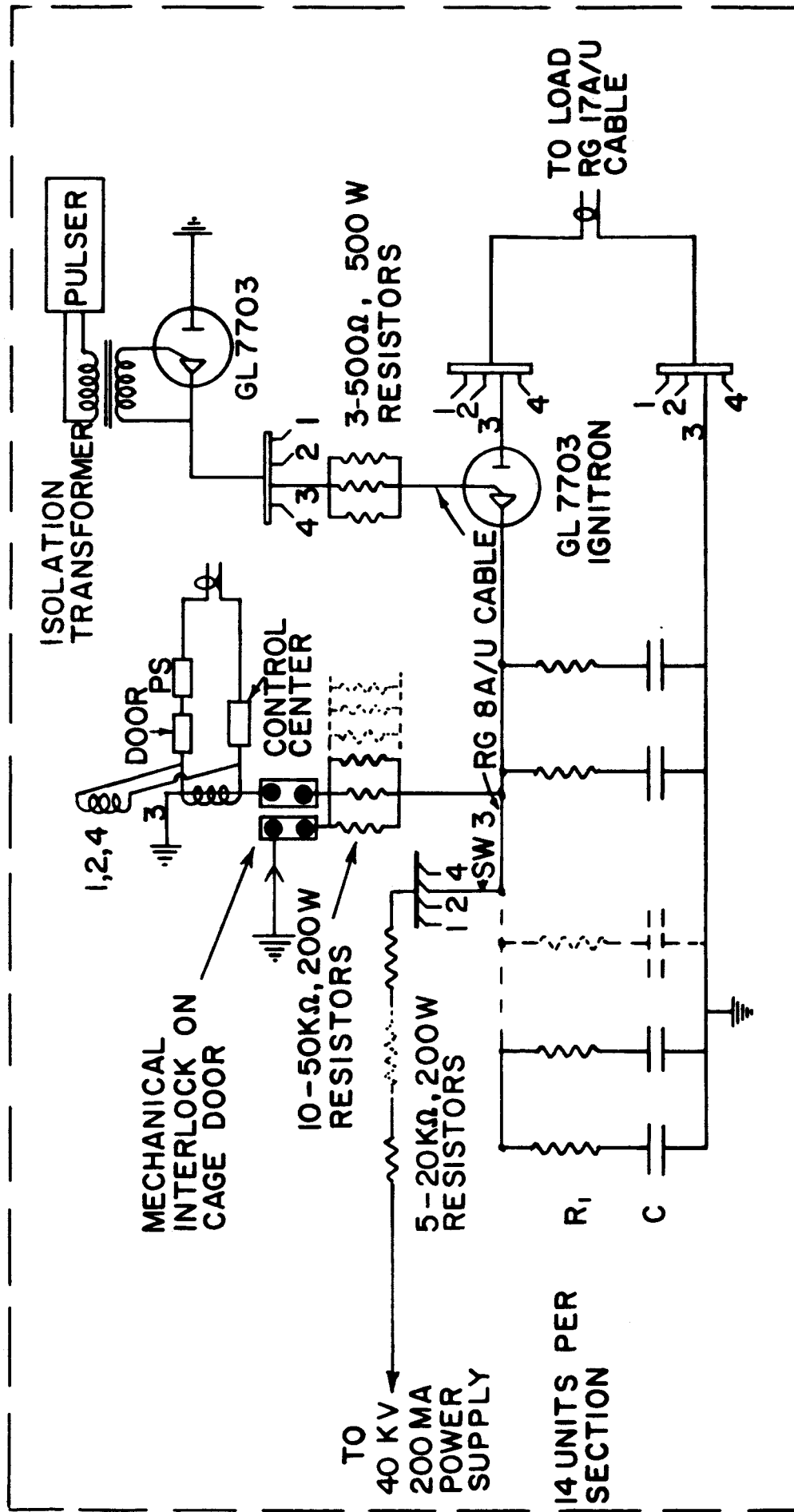
7. Recharging Bank

In anticipation of the evolution of the coaxial gun to a level of performance which would lead necessarily into high repetition-rate tests, the problem of a high voltage, high current power supply became important. The average charging current at a repetition rate of 10^3 shots per second for Mk III or IV would be 50 amperes at 20 kv; such a power supply would be exceedingly expensive and difficult to construct.

On the other hand, any gun which might be similar to the present ones in size, design, and materials, is certainly not capable of sustaining a dissipation in the several hundred kilowatt range for much more than a second. It was felt, then, that a reasonable solution to the power supply requirement would be the use of a bank of capacitors having sufficient stored energy to supply the required current for a few hundred shots, which would be a large enough number to bring the discharge conditions to a steady state.

This bank was constructed during the time other single-shot experiments were in progress on the guns. It consists of 56 units, each 15 μ F, 20 kv which store 168,000 joules of energy. Switching is accomplished by four type 7703 molybdenum-anode ignitrons, each connected to a "shelf" of 14 capacitors. The bank is completely interlocked, both electrically and mechanically, so that personnel access to a charged bank is essentially impossible. Figure 30 is an electrical schematic of the bank, and Figure 31 gives a general view of the installation through the door of the protective cage.

The bank voltage will, of course, drop during a multi-shot run of the gun, and the number of gun firings which may be obtained will be determined by: (1) the acceptable voltage change, and (2) the gun-to-bank capacitance ratio, i.e.,



R_1 — 7.5Ω RESISTOR, 50 MIL NICHROME WIREWOUND

C — AEROVOX CAPACITOR MODEL PX 120J38
20 KV, 15 μ fd

FIG. 30. ELECTRICAL SCHEMATIC OF THE CONDENSER BANK



FIG. 31. THE CONDENSER BANK

$$\frac{\Delta V}{V} = - \frac{C_{\text{gun}}}{C_{\text{bank}}} \cdot \Delta n ,$$

where Δn is an incremental number of shots. This gives

$$n = \frac{C_b}{C_g} \ln \frac{V_o}{V} .$$

For

$$\frac{V_o}{V} = \frac{20\text{kv}}{15\text{kv}} = 1.33, \text{ and}$$

$$\frac{C_b}{C_g} = \frac{840\mu\text{fd}}{5\mu\text{fd}} ,$$

$$n = 48$$

On the other hand, for $C_g = 1 \mu\text{fd}$, and $\frac{V_o}{V} = 2$, we get $n = 580$. The number of shots available will certainly be adequate for presently planned tests.

H. Discussion and Conclusions

In a program such as this one, which involves a particular technical goal, it is worthwhile to review the progress made in terms of progress toward that goal, as well as to enumerate incidental accomplishments in the sense of development of techniques and accrual of generally useful physical data.

This program began with a specific concept of plasma propulsion, i.e., the use of a coaxial gun in the simplest conceivable mode of operation. This mode includes the elimination of as many switches, valves, and other mechanical devices as possible in order to improve reliability, and has consequently centered on the idea of a "relaxation oscillator" type of operation in which both electrical power and propellant would flow uninterrupted into the gun, whose demand for them would be impulsive.

The initial concept also involved a parameter constraint on the storage capacitance, this being determined by the probable attainable

size of a vacuum-electric unit.

These considerations, then, have determined the general design characteristics of the guns used in this work. But, apart from engineering design of a space engine, there exists the far more important and fundamental problem of establishing the feasibility of using MHD for propulsion. It has not been obvious that plasma acceleration can be made efficient; many varieties of energy loss in plasma systems are notoriously well known, and if they cannot be reduced to negligible levels in our device, all engineering questions are irrelevant. We have, therefore, taken the position that the physical questions of the acceleration process are the most important, and should receive the greatest initial attention.

The general set of questions to which this project has addressed itself, then, are roughly these:

1. Can a workable, compatible set of system parameters be found which make efficient plasma acceleration possible?
2. Are there intrinsic physical limitations on the efficiency with which one may impulsively accelerate a plasma?
3. Is the self-oscillating mode of gun firing (no electrical switches or gas valves) feasible?
4. What other design or material problems stand in the way of making a compact, high-power, high repetition-rate engine?

We will summarize our present knowledge of the answers to these questions here.

First, the difficulty of finding a compatible and practical set of system parameters is mainly that of: (1) obtaining very low inductance capacitors and transmission lines, and (2) finding a propellant which will break down at the applied voltage when just the correct mass is in the gun. It appears that if we insist upon limiting C to 1 μfd , we cannot yet obtain a commercial capacitor of low enough inductance, although it is known that some manufacturers (notably Tobe-Deutschmann) are developing

capacitors which are good enough. The further problem of making a vacuum capacitor which itself has low enough inductance may be far more difficult, and has not been dealt with yet. We conclude from the Mark III results that given freedom to vary C , it is indeed possible to obtain a discharge on an optimum gas loading.

It must be strongly re-emphasized that the gun equations, the relation between ℓ , L' , v , and C , and the parameter κ , are at best only rough design guides. While κ , for example, can be interpreted in terms of efficiency if we also assume that the acceleration only proceeds for some certain number (or fraction) of electrical oscillations, such a definition is highly artificial. The real utility of κ is its being a guide to the inter-relationship of system parameters. Efficiency is determined by the relative magnitudes of $\partial L/\partial t$ and the electrical resistance R , and since we have no a priori way of estimating R , (except, perhaps, for a lower limit) we must simply rely on experiment. Nevertheless, it seems desirable to arrange parameters so that no more than one full cycle of the driving current is needed to complete the acceleration.

The answer to question 2 can only be obtained through experiment. While it is well known that many loss mechanisms such as bombardment of electrodes, optical radiation, and instability formation all exist, and will probably occur, the magnitude of their effects is difficult to estimate. It has been mentioned that a short acceleration length should militate against some of these losses. It should be possible experimentally to isolate certain loss channels such as radiation and instability, and also to perform calorimetric measurements on various parts of the gun; however, one is never certain of having identified all the loss modes, and so a more satisfying procedure would be to measure the actual output energy and establish that is a large enough fraction of what was put into the gun.

So far, we have not obtained an output which is a large fraction of the bank energy; however, it seems from Mark III, that we have been able to achieve high efficiency of transfer of field energy to directed plasma energy, since all estimates of the plasma kinetic energy, whether obtained from E_z and n_1 , $\int B^2 dz$, or from the calorimeter, give closely similar results. If these results are borne out by further work, it will constitute

adequate proof that the various losses mentioned above are indeed unimportant.

The feasibility of the free-running continuous gas flow modes of operation (question 3) seems to be in doubt. The de-ionization times we have observed are very long, and have extended into the refill time under free gas flow. It will also be desirable, in periods before large power supplies are available, to make possible much lower repetition rates than the free inflow of propellant would allow. Both of these situations make it seem likely that at least for the immediate future, it will be necessary to use some sort of a repetitively pulsed gas valve. The use of passive circuit elements in the re-charging circuit still seems feasible, and we will continue to assume this mode of electrical operation.

The most important engineering questions posed by question 4 seem to fall into three areas: (1) problems of high-temperature durability and effectiveness of the necessary metals and insulators, including their erosion under discharge conditions, and (2) the design of an adequate energy storage capacitor. We have not improved our knowledge in the first area at all in this work, since so far single-shot operation has been the rule. When a few hundred shots can be fired in rapid sequence, we will know more. This question will not be discussed further.

(3) ?

As to capacitors, there are some developments of interest which should be followed closely. We assumed at the outset of this work that conventional (e.g., oil-paper) capacitors are absolutely ruled out in this application, because of low Q, and this still appears to be true. However, it may not be necessary to go to the full extreme of vacuum dielectric. We have verbal information from the manufacturer of our present capacitors (Axel) that they have done development work on capacitors which employ low-loss dielectrics (at some sacrifice in bulk) together with internal fluid cooling, which in their opinion could come near to meeting our requirement if the gun were run at less than a megawatt. No information was obtained on the attainable inductance of these units, but if the recent work at Tobe Deutschmann (on Los Alamos designs) were incorporated into

a fluid-cooled unit, a solution to our requirement might be in hand.

It is important also to summarize here the more general accomplishments of this program.

We have demonstrated quite clearly that the acceleration of plasma is a complicated process which cannot be interpreted simply in terms of experimental data on luminous fronts, current layers, or even momentum transfer in ballistic pendulum measurements. In connection with this work, we have brought the technique of simultaneous E and B probing to a state of great usefulness. So far as we can determine, it is the only method currently available for the measurement of ion densities and ion momentum transfer in apparatus of this kind, and we are not aware of the technique ever having been employed before.

It has been demonstrated that plasma acceleration by $\vec{j} \times \vec{B}$ forces does not, in general, take place in "snowplow" fashion, but rather through momentum transfer from an ionizing current wave which moves through the plasma.

APPENDIX I

MAGNETIC PROBES-CONSTRUCTION AND CALIBRATION

The B-probes used in this work were of extremely simple design, in that no electrostatic shielding was used on them, and they were not unusual in either their degree of miniaturization or number of turns. Figure 32 is a representation of the probe structure. The coils of most of the probes used for the experiments were 4 to 6 turns of 0.3 mm diameter Formvar-coated wire, wound on a 3 mm diameter form. Just after winding, the coil was slipped off the form and while being held by the leads, dipped into a pot of "minit-cure" epoxy resin, which as the name implies, sets and cures in one minute. The encapsulated coil was then connected directly, and with as short leads as possible, to the end of a miniature coaxial cable, (RG-196) and the assembly inserted into a 5 mm Pyrex glass tube. A flake of black wax was dropped into the closed end of the glass jacket before insertion of the coil and cable, and when the coil had come into place at the tip, the glass was heated so that the wax fastened the coil and jacket together. It was found that the connection of the coax cable directly to the coil was necessary when the very fast rise times encountered in Mark II were being measured. The reason is that a long twisted pair coming out from the coil is a transmission line of different impedance from ordinary cable, and their connection results in a mismatch which has been observed to create cable ringing, seen as "hash". For short probes or moderate rise rates, however, this precaution should not be necessary.

Calibration of the B probes is done by comparison with a single-turn standard coil whose area is large enough to be measured accurately. The comparison is made with the use of a ballistic galvanometer "flip-coil" technique. Each of the coils in turn is connected to a sensitive galvanometer, placed between the poles of a permanent magnet, and quickly withdrawn. Deflection is proportional to coil area, and so a comparison can be made. It is, however, possible to estimate the probe area by the

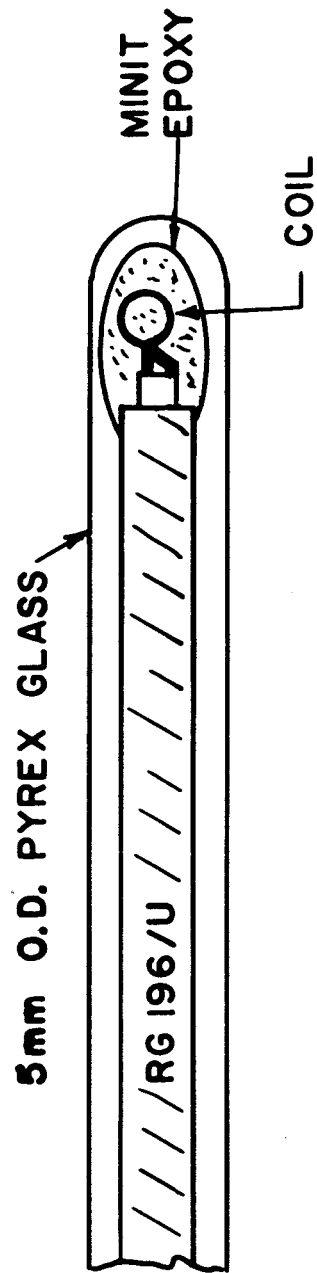


FIG. 32. THE 'B' PROBE

number of turns, coil form area, wire thickness, and certain lead corrections. We found that this determination agreed within 3% with the standard-coil calibration for a 4-turn coil used for obtaining much of the data shown here.

Frequency response of the probe is determined by the time constant L/R , where L is the coil inductance, and R is the impedance of the terminated output line. For the coils employed in this work and the 50 ohm cables connected to them we calculate L/R to be about 10^{-9} seconds, which is almost two orders of magnitude faster rise time than required in the experiment. In other words, we could employ coils with four or five times the number of turns, and still not suffer from inadequate response.

Integration was accomplished with simple RC integrators whose component values were measured on a bridge. A time constant of about 20 μ secs. was used for all of the gun data shown in this report.

APPENDIX II

E-PROBE CONSTRUCTION AND CALIBRATION

Figure 33 shows schematically the E-probe construction. A glass tube was drawn to a thin tip and cut off at a radius which would just pass the braid of an RG-196 coaxial cable. Soft-solder electrodes, a ring and a ball, respectively, were attached to the braid and center conductor, spaced by 1 cm along the cable. The whole assembly was then cast in epoxy resin, and ground to a smooth conical tip, with the exposed electrodes flush with the surface.

Calibration of the E-probe system was done simply by applying the output of a pulser to the tips, and measuring both this voltage and the system output on an oscilloscope. The more difficult operation of balancing the circuits was done by shorting the tips with a symmetrical tab (to avoid inductive pickup) and inserting the probe into the actual gun discharge. Balancing was considered adequate when the residual noise was an order of magnitude less than the expected value of E_z .

The impedance of the output circuit across the probe can be fairly low in these devices. It has been demonstrated here and at Los Alamos⁵ that the probe can be shunted by a very low impedance, a few ohms or less, which can draw hundreds of amperes from the discharge without seriously affecting the signal. Therefore, an input impedance as low as 50 Ω is tolerable.

RG 196 / U

5 mm GLASS

GLASS PULLED 3" LONG

MINIT EPOXY

BRAID

INSULATION

BLACK WAX

FLARED GLASS

OPEN INSULATION
AND BRAID FILLED
WITH EPOXY TO
MAKE VACUUM SEAL

MINIT EPOXY

CENTER WIRE

FIG. 33. THE 'E' PROBE

APPENDIX III

E-PROBE TRANSFORMER

The pair of voltage dividers used between the E-probe and the oscilloscope for the Mark I experiments became inadequate when the Mark II work was started. This inadequacy was not due to the resistors themselves, but rather to the fact that the balanced pre-amplifiers (type G and type Z) used on the oscilloscope lost their balancing at the high signal frequencies (> 10 mc) encountered in the faster gun. It became necessary, then, to resort to a transformer and a single, unbalanced scope input.

A toroidal powdered-iron core was procured which had adequate frequency response. However, first tests of the transformer failed because of excessive common-mode capacitive feed-through. The capacitance was that from each of the windings to the common core. The first step taken to remedy this common-mode response was to space the windings away from the core, and to make them very small, (8 turns of #28 wire, close-spaced). This reduced the feed-through amplitude by a factor of five. The next step was the insertion of a split cylindrical shield between the core and the secondary winding, and the erection of a shield between the two windings. The result was a further common-mode reduction factor of 20, which was enough for our purposes. The primary-to-secondary capacitance, as determined from attenuation of a 35 mc signal, is $0.05 \mu\text{f}$.

Since the coupling of the transformer is not perfect it was necessary to insert a $2.2 \text{ K}\Omega$ resistor in series with the output in order that the series leakage inductance would not degrade the high-frequency response. The resulting attenuation, a factor of 40, was still tolerable, since it had been 100 with the voltage dividers.

The 2.2 K resistance reduced L/R to a point where the input and output transformer pulses rose in times shorter than the 30 mc oscilloscope could display; i.e., the transformer frequency response was better than the experiment required.

Finally, the whole assembly was mounted in a copper shield box and cast in epoxy. The high voltage primary leads emerge through the epoxy surface on the one open side of the box. In operation, the box is only grounded through the shield of the coaxial line which connects its output to the screen room bulkhead. Figure 34 is a schematic drawing of the arrangement of shields and windings on the transformer.

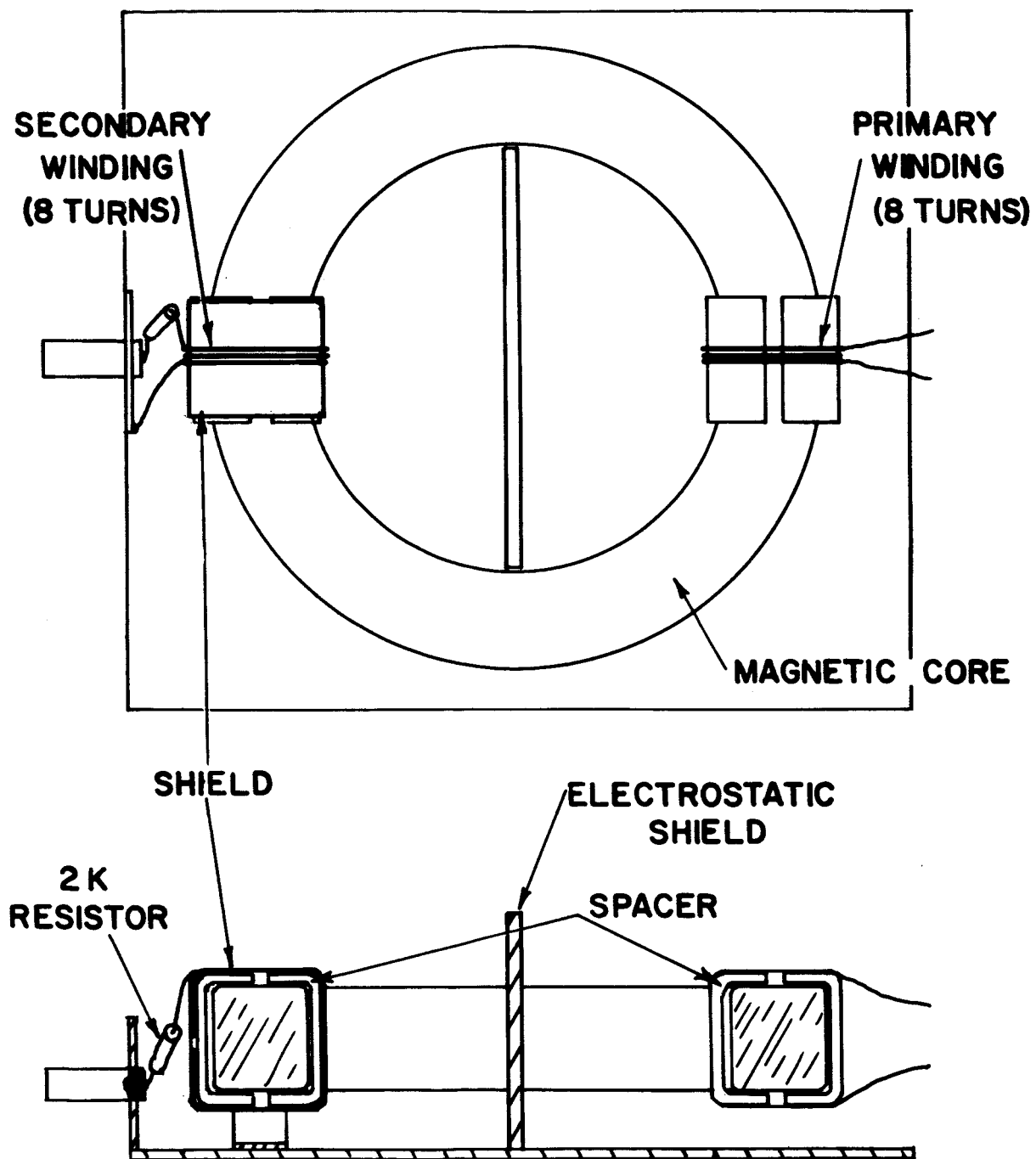


FIG. 34. THE 'E' PROBE ISOLATION TRANSFORMER

APPENDIX IV

EFFECTS OF EXTRANEOUS IMBEDDED MAGNETIC FIELDS

For some time during the initial operation of Mk II, it was noticed that the discharge current was very erratic in azimuthal distribution, even at early times, and that there was a strong tendency toward breakdown prior to introduction of the propellant. The reason was discovered to be that an insert placed inside the center electrode in order to space the gas valve had been made from 400-series stainless steel, which is capable of being magnetized. This particular thin ring was setting up a dipole field transverse to the barrel of about 50 gauss amplitude. The entire episode, counting worthless data runs and the time to search out the trouble, cost three to four weeks of time. The moral, if any, is that the materials used in a device of this sort which is very sensitive to magnetic fields, should be carefully inspected prior to their incorporation into the equipment.

REFERENCES

1. Jensen and Voorhis, General Atomic Report No. 2867
2. R. H. Lovberg, Ann. Physics 8, 311 (1959).
3. S. Glasstone, R. H. Lovberg, Controlled Thermomuclear Reactions, p. 103, Van Nostrand Inc. 1961.
4. I. Langmuir, H. Mott-Smith, General Electric Review, 27, 449, 538, 616, 762, 810, (1924).
5. L. C. Burkhardt, R. H. Lovberg, Physics of Fluids, Vol. 5, No. 3, p. 341, (1962).
6. S. C. Brown, Basic Data of Plasma Physics, John Wiley (1959).